C.3

# LOS ALAMOS SCIENTIFIC LABORATORY

OF THE UNIVERSITY OF CALIFORNIA

LOS ALAMOS, NEW MEXICO

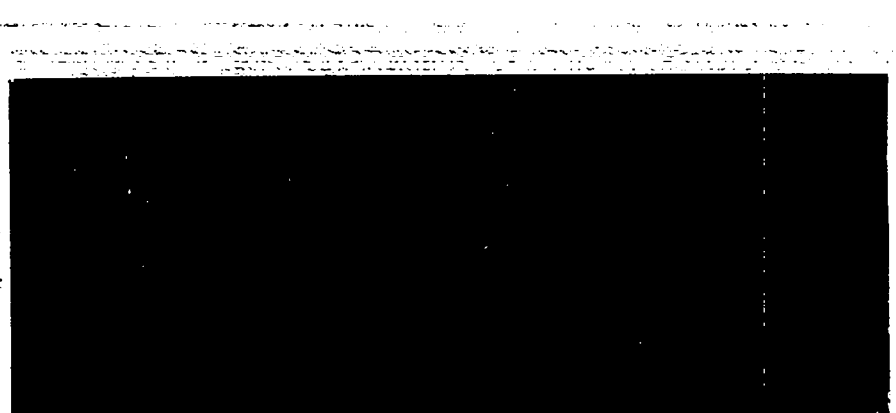



CONTRACT W-7405-ENG. 36 WITH THE
U.S. ATOMIC ENERGY COMMISSION

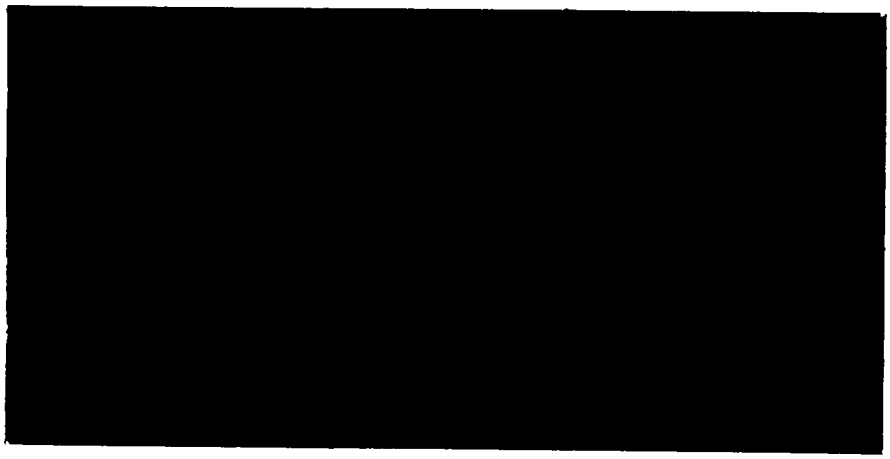

LA-1927

UC-34
Report written: September 1955
Report distributed: May 1956
Report reprinted: December 1976

# Taylor Instability: Appendixes to Report LA-1862

by

Garrett Birkhoff



los alamos
scientific laboratory
of the University of California
LOS ALAMOS, NEW MEXICO 87545

An Affirmative Action/Equal Opportunity Employer

UNITED STATES
ENERGY RESEARCH AND DEVELOPMENT ADMINISTRATION
CONTRACT W-7405-ENG. 36

LOS ALAMOS SCIENTIFIC LABORATORY
of the
UNIVERSITY OF CALIFORNIA

Report written:
September 1955

Report distributed: May 2, 1956

LA-1927

# TAYLOR INSTABILITY
## APPENDICES TO REPORT LA-1862

by

Garrett Birkhoff

PHYSICS

(Distributed according to
TID-4500, 11th edition)

## INTRODUCTION

The material below consists of a more elaborate analysis of various topics discussed in Report LA-1862, "Taylor Instability and Laminar Mixing". These topics are covered in a series of eight appendices, as follows:

## APPENDIX A

## REMARKS ON SIMILARITY

### 1. Analytical Principles

The Similarity Principle described in Sec. 5 of LA-1862 has various obvious extensions. Thus, it applies to liquids in which surface tension is non-negligible, provided the Weber number (Eq. 7 of LA-1862) is the same; it applies to viscous liquids if the Reynolds number (Eq. 8 of LA-1862) is the same, and so on. In the preceding statement, it is, of course, assumed that all non-inertial variables except the one specified are negligible.

To prove the Similarity Principle of Sec. 5, LA-1862, one must also assume that the initial data uniquely determine the solution of Eqs. 3, 4, 6, and 6'. This assumption, though highly plausible, is not trivial; see the discussion at the end of Sec. 22 of LA-1862.

The Impulsive Motion Principle of Sec. 6 of LA-1862 is also hard to prove rigorously, but it can be made plausible as follows. Since the "impulsive velocity" $V = \int_0^T a(t)\,dt$ is assumed bounded, it seems reasonable to suppose that the associated intermediate velocity fields $\nabla U(\vec{x};\, t)$ and $\nabla U'(\vec{x};\, t)$ are also uniformly bounded. Hence the interface displacement should be $O(T)$. Consequently, the acceleration field $\vec{a}(\vec{x};\, t) = \nabla(\partial U/\partial t)$ should differ by $O(T)\, a(t)$ from that $a(t)\nabla A(\vec{x})$ due to an initial acceleration field of strength $a(t)$.

Integrating over the interval $0 \leqq t \leqq T$, we conclude

$$|\nabla U(\vec{x};\ T) - V\nabla A(\vec{x})| \leqq O(T)\int a(t)\,dt = VO(T).$$

Passing to the limit as $T \to 0$, we get the Impulsive Motion Principle.

A third principle, valid for the infinitesimal perturbations discussed in Part II of LA-1862, is the following:

Affine Similarity Principle. Let two initial fluid configurations $\Sigma$, $\Sigma'$ depart initially from horizontal stratification by infinitesimal perturbations $\eta(x,\ z;\ 0)$ and $c\,\eta(x,\ z;\ 0)$. Further, let the Atwood ratio (Eq. 1 of LA-1862) be the same. Then, for all $t > 0$, the interface defining $\Sigma'$ satisfies $\eta'(x,\ z;\ t) = c\,\eta\ (x,z;\ t)$.

This follows simply from the fact that the perturbation equations of Part II are linear. Combined with the Similarity Principle of Sec. 5, it gives a general principle of Froude modeling.

## 2. Wiping and Penetration Coefficients.

Very interesting applications of dimensional analysis can be made to the case of an infinite interface, if it is assumed that perturbations on all scales are equally likely*. The Similarity Principle has important implications, as regards the depth $Y(t)$ of penetration at time $t$. We use the notation of Sec. 8 of LA-1826.

(i) In the case $g = a = 0$ of pure Helmholtz instability, we

*A rigorous treatment of this idea requires statistical methods, and will be deferred to the later report mentioned in the Abstract of LA-1862.

should have

(A1) $$Y = \gamma(u - u')\, t,$$

where the "wiping coefficient" $\gamma$ depends only on the density ratio $\rho'/\rho$ and the degree of initial irregularity.

(ii) In the case $u = u'$ of pure Taylor instability with effective gravity $a - g = ng$, we should have

(A2) $$Y = n\beta\, gt^2,$$

where the "penetration coefficient" $\beta$ also depends only on $\rho'/\rho$ and the initial irregularity.

The prediction (i) has been made by R. Ingraham and J. A. Wheeler in LA-1593, and by E. Frieman in LA-1608, and empirical values $0.1 < \gamma < 0.4$ assigned for the case $\rho = \rho'$. To the empirical evidence given there, may be added the fact* that the turbulent mixing zone of a "half-jet" is well-known to be wedge-shaped, with a vertex angle $2\theta$ of about $30^\circ$, corresponding to $\gamma = 0.25$.

The prediction (ii) corresponds to formula (25) of LA-1862, where $\beta = 0.06$ is deduced for the case $\rho' = 0$. It also corresponds to Taylor's formula $Y_1 = (ng/2)t^2$ for the case of free fall of the "spike into a vacuum.

It should be emphasized that Eqs. A1 and A2 were derived on the assumption that there was inertial modeling and no characteristic

*A brief review of the literature will be given in Ch. XIV of "Jets, wakes and cavities", by G. Birkhoff and E. Zarantonello, to appear in 1956.

wave-length. Thus, they do not apply to the case of a periodic interface of wave-length $\lambda$ .

It should also be noted that, for large t (specifically, when $at >> |u - u'|$), Taylor instability will ultimately dominate Helmholtz instability. This follows since Eq. A1 is linear in t, while A2 is quadratic.

APPENDIX B

INITIAL ACCELERATION

1. Introduction.

In Sec. 6 of LA-1862, the concepts of initial and impulsive acceleration were introduced, and reduced to the following boundary value problem of potential theory, relative to the interface S.

To find functions U and U', harmonic in the regions R and R' separated by S, and satisfying on S

(B1) $\rho U - \rho' U' = \phi(\rho)$, a known function

(B1') $\partial U/\partial n = \partial U'/\partial n$.

Further, U and U' are regular at infinity (for a suitable reference frame).

The present appendix gives a theoretical discussion of the preceding boundary value problem. It is intended to supplement O. D. Kellogg's "Potential Theory" (Ref. 10 of LA-1862), and the 1955 Harvard Doctoral Thesis "Induced Potentials", by James L. Howland*.

*This will be referred to as (JH) in this Appendix. Mr. Howland has also helped in the preparation of the present Appendix.

## 2. Single Layer Potentials.

We first show how to express any solution of the preceding problem in terms of a single layer potential.

In the two-dimensional case of plane flows, this aim is easily accomplished by representing the flow by a vortex layer on S. Such a layer is mathematically equivalent to a single layer for the stream function $V(x,y)$ conjugate to U. Since Eq. B1' is equivalent to $\partial V/\partial s = \partial V'/\partial s$, we can make $V = V'$ on S <u>if</u> S is connected. From Eq. B1, we get similarly

$$(B1^*) \qquad \rho \partial V/\partial n = \rho' \partial V'/\partial n = -\partial \phi/\partial s = \psi ,$$

a known function. Evidently this is a single layer potential (Ref. 10 of LA-1862, p. 287).

In three-dimensional space, it is obvious (Ref. 10, p. 286) that the combined potential field (U,U') in R∪R' can be represented as a <u>double layer</u> potential. Namely, because of the continuity in the normal derivative of U, Eq. B1', (U,U') is the potential of a double layer on S, consisting of a distribution of dipoles normal to S, whose moment per unit area is proportional to U-U', the jump in (U,U') across S.

We now consider the combined field $(V,V') = (\rho U, \rho' U') - (U_\phi, U'_\phi)$, where $(U_\phi, U'_\phi)$ is the field due to a known double layer of intensity $(\rho - \rho')\phi(\vec{x})$. By Eq. B1, (V,V') is continuous across S; hence it is the potential of a <u>single layer</u>, and

(B1**) $\rho' \partial V/\partial n - \rho \partial V'/\partial n = \rho \partial U'_\phi/ n - \rho' \partial U_\phi/\partial n = -\psi$,

a known function of position on S.

## 3. Integral Equation.

Equations B1* and B1** can be transformed into Fredholm integral equations by classical methods. One starts with the Plemelj formulas

(B2) $\partial V/\partial n - \partial V'/\partial n = 2\mu$

(B2') $\partial V/\partial n + \partial V'/\partial n = 2\int K(p,q)\,\mu(q)\,dS_q$

relating the intensity of a single layer $\mu(q)$, with the normal derivatives of the associated potential $V(p)$. Here $K(p,q) = \partial G(p,q)/\partial n_q$ is the Poincaré-Neumann kernel of potential theory, $G(p,q)$ being the Green's function for the pole p.

Thus, if $R \cup R'$ fills the infinite plane, $G(p,q) = (1/2\pi)\mathrm{Ln}\, r(p,q)$. In infinite space, $G(p,q) = 1/4\pi r(p,q)$. For a periodic interface with period $\pi$, in plane motion, $G(p,q) = (1/2\pi)\mathrm{Ln}\sin r(p,q)$, and so on. The case of two liquids with interface S, enclosed in a rigidly accelerated container C, satisfies similar formulas for a generalized Green's function* satisfying $\partial G/\partial n_q = 0$ on C, and so on.

*"Green's function of the second kind",Ref. 10 of LA-1862, or "Neumann function" in the sense of Bergman-Schiffer, "Kernel functions...". For a discussion of such more general cases, see Howland's Thesis.

Adding $(\rho + \rho')/2$ times Eq. B2 to $(\rho - \rho')/2$ times Eq. B2', and substituting in Eq. B1*, we get

$$(B3) \qquad \mu(p) + \alpha \int K(p,q)\,\mu(q)dq = \psi_1(p),$$

where $\alpha = (\rho - \rho')/(\rho + \rho')$, as in LA-1862. Substituting in Eq. B1**, we get

$$(B3') \qquad \mu(p) - \alpha \int K(p,q)\,\mu(q)dq = \psi_2(p).$$

Finally, Eq. 6 of LA-1862 reduces to another equation of the same form.

Thus, in all cases, we get a Fredholm integral equation, where $-1 \leqq \alpha \leqq 1$ since $\rho$ and $\rho'$ are non-negative. We shall now exploit this fact, giving relevant interpretations of the formulas.

First, we recall Fredholm's basic formula for solving Eq. B3',

$$(B4') \qquad D(\alpha)\,\mu(p) = \int D(p,q;\alpha)\,\psi_2(q)\,dS_q .$$

Here $D(p,q;\alpha) = \sum_0^\infty (-\alpha)^n C_n(p,q)$ corresponds to the matrix of minors ("adjoint") of $I-\alpha K(p,q)$, and is an entire function of the complex variable $\alpha$. The Fredholm determinant $D(\alpha)$, which corresponds to $|I-\alpha K|$ in the matrix analog, is another entire function. Clearly, the series B4' solves B3' except when $D(\alpha) = 0$. The exceptional eigenvalues $\alpha = \alpha_i$ for which $D(\alpha) = 0$ should be considered as the reciprocals $\alpha_i = \gamma_i^{-1}$ of the eigenvalues $\gamma_i$ of $K(p,q)$. Since $D(\alpha)$ is an entire function, it has only a finite number of zeros inside any

circle $|\alpha| < R$.

Identical formulas, but with $-\alpha$ replaced by $\alpha$, hold for Eq. 3. Thus,

$$(B4) \qquad D(-\alpha)\mu(p) = \int D(p,q;-\alpha)\ \psi_1(q)dS_q \ .$$

Finally, analogous formulas hold for the double layer representation, but with $K(p,q)$ replaced by $K(q,p)$, and $D(p,q;\alpha)$ replaced by its transpose $D(q,p;\alpha)$. The same $D(\alpha)$ occurs, whence the integral equation for the intensity of the double layer has the same eigenvalues.

## 4. Dirichlet Integral.

By the Dirichlet integral of the combined potential $(V,V')$ due to a single layer $\mu$ on S, is meant the scalar

$$(B5) \qquad \int_R \nabla V \cdot \nabla V \, dR + \int_{R'} \nabla U' \cdot \nabla U' dR' \ .$$

By Green's theorem*, this is also equal to

$$(B5') \qquad \int_S V \frac{\partial V}{\partial n} dS + \int_S V' \frac{\partial V'}{\partial n'} dS = \int_S V\left(\frac{\partial V}{\partial n} - \frac{\partial V'}{\partial n}\right)dS \ .$$

(Since $\frac{\partial G}{\partial n}(p,q) = 0$ on C, this formula also holds for the case of a finite container.) Hence, by Eqs. B2 and B2', the integral equals

*In the plane, the integral (5) will not converge unless $\int \mu dS = 0$.

(B5") $$k \int_S \mu(p) G(p,q) \mu(q) d\,S_p d\,S_q = 2[\mu, \mu],$$

where $k = \pi^{-1}$ in the plane, and $k = (2\pi)^{-1}$ in space. Finally, since $G(p,q)$ is bilinear, symmetric, and positive definite, the "norm" $[\mu, \mu]$ defines a Hilbert space $\mathcal{H}$ of single layer distributions on S.

In summary, we have constructed a Hilbert space, the square of whose norm equals the Dirichlet integrals B5 and B5'. It is also a special case of the inner product

(B6) $$[\mu, \nu] = (\mu G, \nu) = (\mu, \nu G)$$

$$= \frac{1}{2} \int_S \left(U \frac{\partial V}{\partial n} + U' \frac{\partial V'}{\partial n}\right) dS$$

$$= \frac{1}{2} \int_R \nabla U \cdot \nabla V \, dR + \frac{1}{2} \int_{R'} \nabla U' \cdot \nabla V' \, dR'.$$

This inner product is very useful mathematically.

The Dirichlet integral $2[\mu, \mu]$ has well-known physical interpretations. If $\rho = \rho'$, then clearly $[\mu, \mu]$ expresses the kinetic energy associated with the flow with velocity potential (U,U'). In the case of plane flow with stream function (V,V'), $[\mu, \mu]$ also expresses the kinetic energy of the flow associated with the vortex layer $\mu(p)$. Again, in the electrostatic interpretation (see Sec. 8 of LA-1862), consideration of Eq. B5' or B5" shows that $[\mu, \mu]$ is proportional to the potential energy of the given charge distribution. (In the case of a

"container" C, $[\mu,\mu]$ is the potential energy in the presence of the grounded conductor). Similarly $[\mu,\nu]$ represents the interaction energy of two charge distributions.

The Dirichlet integral corresponds to two variational principles for fluid motion. The first is due in principle to Kelvin*. It asserts that, in the case of fluid of variable density filling an accelerated container C, the actual fluid motion minimizes the total kinetic energy, relative to all other volume-conserving flows. Unfortunately, in the most interesting case of an infinite fluid, it seems difficult to formulate an analogous Minimum Principle.

However, one can formulate a dual Maximum Principle by referring the motion to moving axes, making the mean interfacial acceleration zero. (This corresponds to replacing acceleration by a virtual gravity field.) Namely, one can show that the actual fluid motion maximizes the conversion of potential into kinetic energy, relative to all other flows which conserve both volume and energy. This result can be considered as an extension of Bertrand's Theorem** to the case of Lagrangian systems with infinitely many degrees of freedom.

## 5. The Operator K.

The Hilbert space $\mathcal{H}$ defined in Sec. 3 greatly simplifies the analysis of the linear operator K: $\mu(p) \rightarrow \int K(p,q)\,\mu(q)\,dS_q$ defined in

*See G. Birkhoff, Quar. Appl. Math. 10 (1952), 81-6 and 11 (1953), 109-10.

**E. T. Whittaker, "Analytical Dynamics", Cambridge University Press, 4th ed., 1937, Sec. 108.

Sec. 2. Thus, if V and W are the potentials $G\mu$, and $G\nu$ defined by the single layers $\mu$ and $\nu$, then, since $\partial/\partial n' = -\partial/\partial n$, Eqs. B2 and B2' imply

$$(B7) \qquad [\mu,\nu] = \iint \left[\frac{\partial V}{\partial n}(p) + \frac{\partial V'}{\partial n'}(p)\right] G(p,q)\nu(q)dS_p dS_q$$

$$= \int \left[\frac{\partial V}{\partial n} + \frac{\partial V'}{\partial n'}\right] W\, dS_p .$$

$$(B7') \qquad [\mu K,\nu] = \iint \left[\frac{\partial V}{\partial n}(p) - \frac{\partial V'}{\partial n'}(p)\right] G(p,q)\nu(q)dS_p dS_q$$

$$= \int \left[\frac{\partial V}{\partial n} - \frac{\partial V'}{\partial n'}\right] W dS_q .$$

Now applying Green's identity to Eq. B7', we get

$$(B8) \qquad [\mu K,\nu] = \int_R (\nabla V\cdot\nabla W)\, dR - \int_{R'} (\nabla V'\cdot\nabla W')\, dR'$$

$$= [\mu,\nu K],$$

which is also directly related to the Dirichlet integral.

Hence, we can regard K as a symmetric operator on $\mathcal{H}$. Moreover, Eq. B7 can be similarly rewritten

$$(B8') \qquad [\mu,\nu] = \int_R (\nabla V\cdot\nabla W)dR + \int_{R'} (\nabla V'\cdot\nabla W')dR'.$$

Comparing with Eq. B8, and noting that both terms are positive if $V = W$, we get

(B9) $$[\mu K, \mu] \leqq [\mu, \mu] \ .$$

From this it follows that*

(B9*) $$[\mu K, \mu K] \leqq [\mu, \mu] \ ;$$

K is a contraction of $\mathfrak{H}$ , in the usual sense.

Theorem 1. The bounded symmetric operator K has a discrete spectrum. Hence $\mathfrak{H}$ contains an orthonormal basis of eigenfunctions $\mu_i$, such that

(B10) $$\mu_i K = \lambda_i \mu_i \qquad (-1 \leqq \lambda_i \leqq 1).$$

Proof. For a suitable "resolution of the identity" into permutable projections $E_\lambda$,

$$K = \int_{-1}^{1} \lambda dE_\lambda ,$$

by the basic theory of bounded symmetric operators. Again, the mth power (iterate) $K^m$ of K is

$$K^m = \int_{-1}^{1} \lambda^m dE_\lambda .$$

From this it follows that K has a discrete spectrum if and only if $K^m$

*M. H. Stone, "Linear transformations in Hilbert space", New York, The American Mathematical Society, 1932, Thm. 2.21. The proof of Thm. 1 relies on results in this book.

has a discrete spectrum.

Again, if any $K^m$ is completely continuous, then $K^m$ necessarily has a discrete spectrum; hence so does K. But it is classic that if the point-function $K^m(p,q)$ is continuous on a compact set, then the associated operator is completely continuous. Further, in two dimensions, $K(p,q)$ is itself continuous, while in space, $K^3(p,q)$ is continuous (Ref. 10 of LA-1862).

6. Eigenfunctions of K.

The eigenfunctions $\mu_i$ of K, defined by Eq. B10, have various interesting properties. As usual for symmetric operators, eigenfunctions having distinct eigenvalues are orthogonal.

Again, by Eqs. B2 and B2', rewritten as

$$\text{(B11)} \qquad \partial V/\partial n = \mu + K\mu, \quad \partial V'/\partial n' = \mu - K\mu \ ,$$

we see that, if $V_i$ is the potential of the eigenfunction $\mu_i$, with eigenvalue $\lambda_i$, then

$$\text{(B12)} \qquad \partial V_i/\partial n = (1 + \lambda_i)\mu \quad \text{and} \quad \partial V'_i/\partial n' = (1 - \alpha_i)\mu$$

are linearly dependent. Using Eqs. B2 and B2', one can show that, conversely $\beta_i \, \partial V_i/\partial n = \beta'_i \, \partial V'_i/\partial n'$ implies that $\mu_i$ is an eigenfunction of K.

The preceding formulas refer to a vortex layer; in the case of an induced acceleration potential in space, the signs of the $\alpha_i$

are reversed. In either case, the $V_i$ are just the so-called Poincaré fundamental functions. Moreover, if any two of the four functions

$$\mu,\ K\mu,\ \partial V/\partial n,\ \partial V'/\partial n'$$

are proportional, then all four are proportional.

This is clearly one property of spherical harmonics, if S is a sphere; thus the Poincaré fundamental functions for a sphere are the spherical harmonics. The fact that V is proportional to $\partial V/\partial n$ in this case is clearly atypical. If S is a sphere, since there are 2n+1 harmonics of order n, there are $(n+1)^2$ of order $\leq n$; moreover $\lambda = 1/(2n+1)$. This shows that $\lambda_k = O(\sqrt{1/k})$, in this case; this may be typical for surfaces of general shape.

It follows by Thm. 1 that the fundamental functions $V_i(p)$ on S are a complete orthonormal set relative to the inner product $[\mu,\nu]$ of Eq. B7.

We next show that, if $\lambda_i \neq 1$ is an eigenvalue of K in the plane case, then so is $-\lambda_i$. Namely, from Eq. B12, if (V,V') is a Poincaré fundamental function, then the conjugate functions (U,U') satisfy

$$\frac{\partial U}{\partial s} = \frac{\partial V}{\partial n} = \frac{1+\lambda_i}{1-\lambda_i}\frac{\partial V'}{\partial n'} = \frac{1+\lambda_i}{1-\lambda_i}\frac{\partial U'}{\partial s}$$

by Eq. B12. Hence, U and U' can be made proportional to each other. Moreover, since V = V' on S, the combined field (U,U') satisfies

$\partial U/\partial n = \partial V/\partial s = \partial V'/\partial s = \partial U'/\partial n$, and so can be obtained from a double layer potential on S. But the eigenvalues for the latter are those of K(q,p), and hence are the same as those of K(p,q). The result now follows.

## 7. Eigenvalues of K.

We now show that every eigenvalue of K satisfies $-1 < \lambda_i < 1$, except for a single degenerate eigenvalue $\lambda_o = 1$ of multiplicity one, which does not correspond to a solution of the impulsive acceleration problem.

The degenerate eigenvalue $\lambda_o = 1$ corresponds to the solution of the conductor problem $U_o = 1$ in R, whence $\partial U_o/\partial n = O(\partial U_o/\partial n')$. In the case of a vortex distribution, it corresponds similarly to pure circulation around R. In either case, if $\mu_o$ is the density of the corresponding single layer, then $[\mu_o,\mu] = 0$ is equivalent to

$$(B13) \qquad 0 = \int U_o \frac{\partial U}{\partial n}\, dS, \text{ or } \quad 0 = \int \frac{\partial U}{\partial n}\, dS, \text{ or } \quad 0 = \int \mu\, dS.$$

Because of the invariance of circulation, this condition is always satisfied in the case of Taylor instability with zero initial circulation. (This is also true in the case of a periodic plane motion.)

Since $-1 < \lambda_i < 1$ if Eq. B13 holds, it is clear that Eqs. B3 and B3' can be solved by simple iteration in this case, even if $\alpha = 1$ in Eq. B3. In general, the convergence factor will be $|\lambda_1 \alpha|$, where $\lambda_i$ is the eigenvalue $\lambda_i \neq \lambda_o$ of K having the largest magnitude,

and $\alpha = (\rho - \rho')/(\rho + \rho')$.

Estimates of $\lambda_1$ can be made in the plane case, using quasi-conformal mapping*. Extensions of this technique to the case of a periodic boundary would probably be fruitful; in the case of a plane interface, $\lambda_1 = 0$.

If $|\lambda_1| = 1 - \epsilon$ is known, then one can speed up convergence by using polynomials giving a "best possible" approximation to $(1 \pm \alpha K)^{-1}$ on $-\lambda_1 \leqq K \leqq \lambda_1$. A discussion of this has been given recently by Stiefel**.

Iteration of Chebycheff polynomials seems to provide a satisfactory compromise.

[Since writing Appendix B, I have discovered a relevant article by A. Hammerstein, Math. Zeits. 27 (1928), 269-311, in which the completeness of the eigenfunctions of potential theory is also proved by a different method.]

---

*See L. V. Ahlfors, Pac. J. Math. 2 (1952), 271-80.

**E. Stiefel, "On solving Fredholm integral equations", unpublished MS. submitted to the Journal of S.I.A.M.

## APPENDIX C

## STABILITY OF HETEROGENEOUS FLUIDS

Much of the analysis originally intended for Appendix C has appeared elsewhere:

S. Chandrasekhar, "The character of the equilibrium of an incompressible heavy viscous fluid of variable density", Proc. Camb. Phil. Soc. 51 (1955), 162-78.

S. Chandrasekhar, "The character of the equilibrium of an incompressible fluid sphere of variable density and viscosity, subject to radial acceleration", Quar. J. Mech. Appl. Math. 8 (1955), 1-21.

Therefore, Appendix C will be omitted.

APPENDIX D

STEADY STATE BUBBLE RISE*

1. The Problem.

In Sec. 15 of LA-1862, we reviewed the extensive literature treating the rise of a bubble in a cylindrical tube. The present appendix deals with the analogous problem of plane bubble rise in a vertical channel (Fig. 1a). We first treat the question theoretically.

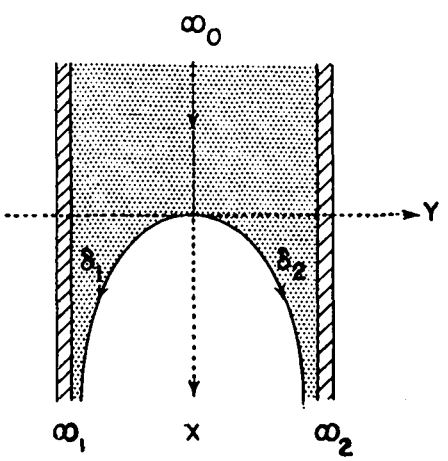


Fig. 1a

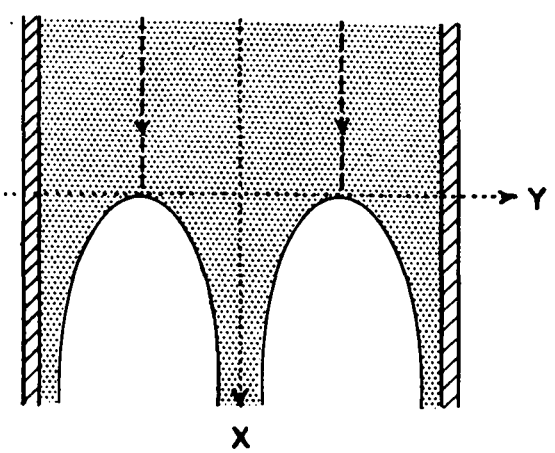


Fig. 1b

We assume steady state motion, relative to axes moving with constant velocity $u_o$ (the bubble rise velocity). Further, we assume that the vector velocity is parallel to a fixed vertical (x,y)-plane, and independent of the third coordinate. We also assume the fluid to be non-viscous. Consequently, we can assume that there is a complex

*Written jointly with David Carter of Los Alamos Scientific Laboratory.

potential $W = U + iV$, depending analytically on complex position $z = x + iy$, such that

(D1) $$dW/dz = u - iv = \zeta(z)$$

is the conjugate complex of the velocity vector $\zeta^* = u + iv$.

We also assume constant pressure in the bubble. This implies that

(D2) $$|\zeta^2(z)| = \zeta\zeta^* = 2gx,$$

where $x$ is the vertical distance below the assumed unique stagnation point, and $g$ is the acceleration of gravity.

It is not obvious that this problem has a solution. Without the extra assumption that the bubble is connected, it is clear that the solution will not be unique: we could have a double bubble rising instead, as in Fig. 1b.

Assuming a single symmetric bubble, however, it may be hoped on physical grounds that the problem just stated has a unique solution. If $R$ is the radius of curvature at the bubble vertex (stagnation point) $z = 0$, and $D$ the diameter of the channel (tube), it will follow by similarity considerations that the two dimensionless ratios

(D3) $$u_o/\sqrt{gD} \qquad \text{and} \qquad R/D$$

will be unique dimensionless constants. Their predicted values can then be compared with experiment.

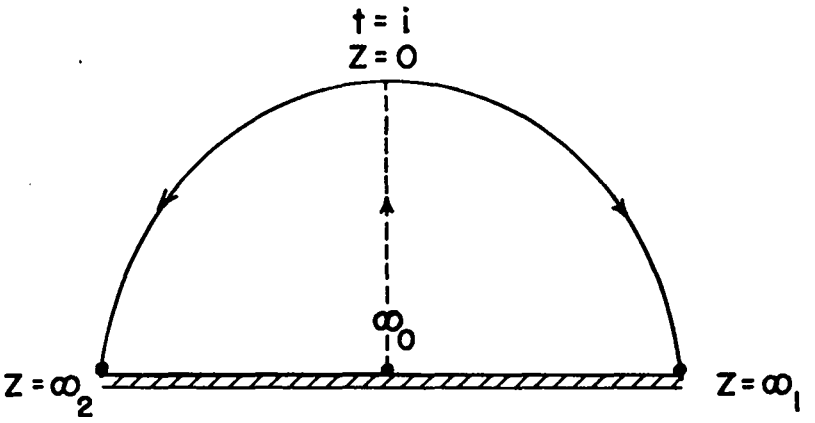


Fig. 2

2. The Function W(t).

Consider an unknown function t(z) which maps the interior of the fluid conformally onto the interior of the unit semi-circle $\Gamma$, as in Fig. 2, so that $\infty_0$ goes onto t = 0, the channel walls on the real diameter, and the bubble vertex on t = i.

Let W be the complex potential, so that

(D4) $$\zeta = \frac{dW}{dz}$$

is the conjugate velocity in the z-plane. If $u_o$ is the fluid velocity at $\infty_o$ in the z-plane ("bubble rise" velocity), then the stream function V(z) has a jump of $u_o D$ across $\infty_o$ counter-clockwise, and equal jumps of $-u_o D/2$ across $\infty_1$, $\infty_2$. Otherwise, V(z) is constant on the boundary.

In the t-plane, V is correspondingly piecewise constant on the boundary of $\Gamma$, except for jumps of $-u_o D/2$ at $t = \pm 1$, and a jump of $u_o D$ at $t = i$. But, apart from a complex additive constant, there is only one function W(t) whose imaginary part V(t) has these properties and merely logarithmic singularities. It is

$$(D4^*) \qquad W = A \operatorname{Ln} \frac{t}{1-t^2}, \qquad \text{where} \quad A = u_o D/\pi > 0.$$

Indeed, on $0 < t < 1$, W is real and so $V = 0$; on $-1 < t < 0$, $v = \pi A$, while on $t = e^{i\sigma}$ ( $\delta_1$ and $\delta_2$),

$$(D5) \qquad W = A \operatorname{Ln} \frac{e^{i\sigma}}{1-e^{2i\sigma}} = -A \operatorname{Ln}(2 \sin \sigma) + iA\pi/2.$$

Hence Eq. D4* gives W(t).

## 3. The Function $\varphi(t)$.

Next we consider the function $\varphi(t)$. Clearly it is real on the real axis, and continuous except at $t = \pm 1$, where it becomes infinite. Hence, by the Schwarz reflection principle, it can be uniquely extended to an analytic function in the unit circle ( $\Gamma$ plus its mirror image). In other words, $\varphi(t)$ can be expanded in a power series with real coefficients, convergent in the unit circle $|t| < 1$.

Physically, the extension by reflection corresponds to reflecting the configuration in the channel walls, so as to obtain an

infinite periodic sequence of rising bubbles. The fact that $t = 0$ is a branch point for $W(t)$, with period $2\pi A$ by Eq. D4, corresponds to the horizontal bubble spacing.

We have assumed that $z = 0$, $t = i$ is the only stagnation point. But, in general

$$(D6) \qquad \zeta = \frac{dW}{dt} \cdot \frac{dt}{dz} = \frac{A(1 + t^2)}{t(1 - t^2)} \frac{dt}{dz} \quad \text{in } \Gamma \ .$$

Hence letting $z'(i) = -iB \neq 0$, we have

$$(D7) \qquad \zeta/(1+t^2) \longrightarrow A/2B \quad \text{as} \quad t \longrightarrow i.$$

This describes the behavior of $\zeta$ near $t = i$. By reflection symmetry, $\zeta$ will also have a simple zero at $t = -i$, and no other zero in $|t| \leqq 1$.

4. Asymptotic Jet Behavior.

We now try to determine the asymptotic behavior of $\zeta(t)$, as $t$ approaches $\pm 1$ along the descending jets, up to a bounded factor. Since the fluid is in free fall near $\infty_1$ and $\infty_2$, $dW/dz = \zeta \sim \sqrt{2gz}$ asymptotically as $t \longrightarrow \pm 1$. Hence $W \sim \int \sqrt{2gz}\, dz = \sqrt{8g}\, z^{3/2}/3$. But again, by Eq. D4*, since $\operatorname{Ln} 2(1 \mp t) \sim \operatorname{Ln} (1 \mp t)$ as $t \longrightarrow \pm 1$, we have

$$W = A \operatorname{Log} \frac{t}{(1\pm t)(1\mp t)} \sim A \operatorname{Ln} \frac{1}{2(1\mp t)} \sim -A \operatorname{Ln} (1 \mp t).$$

Substituting back, we get

(D8a) $$z \sim (3W/\sqrt{8g}\,)^{2/3} \sim \left[\frac{-3A}{\sqrt{8g}} \operatorname{Ln}(1 \mp t)\right]^{2/3}$$

(D8b) $$\zeta \sim \sqrt{2gz} \sim [-3Ag \operatorname{Ln}(1 \mp t)]^{1/3} .$$

Consequently, if $0 < C < 0.5$, then the ratio

$$f(t) = \zeta(t)/(1+t^2)\,[-\operatorname{Ln} C(1-t^2)]^{1/3}$$

is bounded away from zero and infinity throughout $\Gamma$. We have already discussed the behavior near $t = \pm 1, i$; elsewhere, $0 < |C(1-t^2)| \leq 2C < 1$. It follows that we can write

(D9) $$\zeta = (1 + t^2)\,[-\operatorname{Ln} C(1 - t^2)]^{1/3}\, e^{\Omega(t)}, \text{ if } 0 < C < 0.5,$$

where $\Omega(t) = \Omega(t,C)$ is bounded and continuous in the closure of $\Gamma$, and analytic in the interior.

Our solution of the mathematical problem stated in Sec. 1 will consist in the approximate calculation of $\Omega(t,C)$.

5. The Function $\Omega(t,C)$.

Like $\zeta(t)$, the function $\Omega(t,C)$ defined by Eq. D9 is, for any fixed C, real and positive on the real diameter. Moreover it is analytic in $|t| < 1$, and continuous on the boundary $|t| = 1$. Therefore, $\Omega(t,C)$ can be expanded in a power series with real coefficients

(D9*) $$\Omega(t,C) = a_o(C) + a_2(C)t^2 + a_4(C)t^4 + \ldots ,$$

which is certainly convergent for $|t| < 1$, and almost certainly convergent for $|t| \leqq 1$. If we can determine the $a_{2k}(C)$ approximately, for even one C, then we will have determined the flow by Eqs. D9 and D4, and the converse $z = \int \zeta^{-1} dW$ of Eq. D1.

To illustrate this, and for future reference, we shall now apply this principle to express $u_o$, D, g, and B in terms of A, C, and the $a_{2k}$.

At $t = 0$, clearly $\zeta = u_o$; hence by Eqs. D9 and D9*

(D10) $$(-\text{Ln } C)^{1/3} \; e^{a_o} = u_o .$$

This expresses the rate of bubble rise.

We next consider the asymptotic behavior as $t \longrightarrow 1$ (that as $t \longrightarrow -1$ follows by symmetry). Clearly

$$\text{Ln } C(1-t^2)/\text{Ln}(1-t) = 1 + \left[\text{Ln } C(1+t)/\text{Ln } (1-t)\right] \longrightarrow 1.$$

Hence, by Eq. D8b, letting $t \longrightarrow 1$,

$$1 \sim \frac{\zeta}{[-3Ag \; \text{Ln}(1-t)]^{1/3}} \sim \frac{(1+t^2)e^{\Omega(t)}}{[3Ag]^{1/3}} \sim \left[\frac{8}{3Ag}\right]^{1/3} e^{\Omega(t)} .$$

We therefore get the asymptotic relation

(D11) $$a_o + a_2 + a_4 + \ldots = \frac{1}{3} \ln (3Ag/8).$$

Finally, near the bubble vertex, as $t \longrightarrow i$,

$$\mathcal{L}/(1+t^2) \longrightarrow (-\ln 2C)^{1/3}\, e^{a_o - a_2 + a_4 - \cdots} .$$

Comparing with Eqs. D7 and D9, we get the relation

(D12) $$B = iz'(i) = \operatorname{Lim} \frac{(1+t^2)A}{2\mathcal{L}} = \frac{A}{2(-\ln 2C)^{1/3}\, e^{\Omega(i)}} .$$

$$= (Ae^{-a_o + a_2 - a_4 + \ldots})/2(-\ln 2C)^{1/3} .$$

The dimensionless ratio $u_o^2/gD$ is especially interesting (cf. Eq. D3), because it is independent of the choice of units. By Eqs. D4, D10, and D11, we get

(D13) $$u_o^2/gD = u_o^3/\pi gA = (-\ln C)e^{3a_o}/\pi gA$$

$$= 3(-\ln C)/8\pi e^{3a_2 + 3a_4 + \ldots} .$$

We shall now normalize to the case $a_o = 0$, $A = 1$ by choice of space and velocity units. For each choice of C, $0 < C < 0.5$, we will then have

(D14a) $$u_o = (-\ln C)^{1/3}$$ by (D10),

(D14b) $$D = \pi A/u_o = \pi/(-\text{Ln } C)^{1/3} \qquad \text{by (D4*)},$$

(D14c) $$g = (8/3)e^{3(a_2+a_4+\ldots)} \qquad \text{by (D11)},$$

(D14d) $$B = e^{a_2-a_4+\ldots}/2(-\text{Ln } 2C)^{1/3} \qquad \text{by (D12)}.$$

Note that gA and $a_o$ cannot both be specified in advance for given C, as they would determine $u_o$ by Eq. D10, hence D by Eq. D4, and so the dimensionless ratio $u_o^2/gD$, of Eq. D13.

With the preceding normalization, we thus have to compute the constants $a_2, a_4, a_6, \ldots$ . To do this, we must invoke the exact "free boundary" condition, which has not been invoked up to now except in asymptotic form.

## 6. Digression: The Parameter C.

A more careful study of the asymptotic behavior of the "free jet" near $t = \pm 1$, indicates that C should <u>not</u> be taken arbitrarily in the interval $0 < C < 0.5$. C corresponds asymptotically to a constant addend $W_1$ (cf. Eq. D5) in the formula

(D15) $$\zeta \sim K(W-W_1)^{1/3}, \qquad W \sim A \text{ Ln } \pm(1-t^2) .$$

We shall now show that there is just one value of $W_1$ which gives a highest order of approximation in Eq. D9--i.e., makes $\zeta$ as smooth as possible.

Reflecting in the fixed wall, and translating the origin so as to make one branch of the jet fall along the real axis, we try the expansion

$$\text{(D16)} \qquad \zeta = \sqrt{2gz}\,\left(1 + \frac{b_1}{z^{\alpha}} + \frac{b_2}{z^{2\alpha}} + \ldots\right), \quad a_i \text{ real},$$

noting the "free boundary" condition

$$\text{(D16a)} \qquad |\zeta|^2 = 2gx \quad \text{on} \quad z = x \pm i\pi A/\sqrt{8gx}\ .$$

Substituting from Eq. D16 into D16a, we get

$$\text{(D16b)} \qquad 2g|z| \cdot \left|\left(1 + 2b_1/z^{\alpha} + \ldots\right)\right| = 2gx$$

on $z = x(1 \pm i\pi A/\sqrt{8gx^3}\ )$.

But, on $z = x(1 \pm ikx^{-3/2})$, $|z| = |x|\,(1 + k^2/2x^3 + \ldots)$.

Hence $|1 + 2b_1/z^{\alpha} + \ldots| = (1 + k^2/2x^3 + \ldots)^{-1}$, and

$$\text{(D16*)} \qquad \zeta = \sqrt{2gz}\,(1 + b_1/z^3 + \ldots).$$

Integrating

$$\text{(D17)} \qquad W = \int \zeta\, dz = \frac{\sqrt{8g}}{3}\, z^{3/2} + W_1 + O(z^{-3/2}),$$

for some constant $W_1$. This justifies Eq. D15.

If the right C is used, then

$$\text{(D18)} \qquad \zeta/(W-W_1)^{1/3} \sim K + O(z^{-3}) \sim K + O(W^{-2})$$

$$\sim K + \left[\,\mathrm{Ln}(1-t^2)\,\right]^{-2}.$$

Otherwise, since $(W-W_1)^{1/3}/W^{1/3} = 1 + O(W^{-1})$, it would appear that the asymptotic approximation has a lower order of accuracy.

It would seem that, with care, condition (D18) could be converted into an asymptotic equation at $\sigma = 0, \pi$ (one equation by symmetry) involving C, which could be used to determine C. Our numerical experience suggests that $2C = 1/e$ is not far from the correct value. However, considerable formal analysis would be required to obtain such a condition in its most elegant form.

It is not clear whether or not such a condition on C is necessary or sufficient to make equally spaced interpolation converge*, as $n \longrightarrow \infty$, using the method of Sec. 9. However, it would seem to help substantially in obtaining accurate approximations for small n.

## 7. Free Boundary Condition.

To interpret the free boundary condition, we write $\zeta = ve^{i\phi}$, so that $v = |\zeta|$ is the velocity magnitude, and $-\phi = -\arg \zeta$ its direction. On the free streamline $t = e^{i\sigma}$, the free boundary condition is $v^2 = 2gx$.

Since $v = 0$ when $t = i$, by Eq. D9, this is equivalent to $vdv/ds = \pm g \cos \phi$ on $t = e^{i\sigma}$. Again, since $dW/ds = v$, clearly $d\sigma/ds = v\, d\sigma/dW$, and so the free streamline condition may be taken as

*Cf. Dunham Jackson, "Theory of approximation", New York, The American Mathematical Society, 1930, p. 123, Cor. 2.

$$v^2 \frac{dv}{d\sigma} \frac{d\sigma}{dW} = g \cos \phi \ .$$

But again, on $t = e^{i\sigma}$, by Eq. D5, $dW/d\sigma = -A \cot \sigma$. Substituting in the preceding equation, we get (normalizing to $A = 1$),

(D19) $$\frac{1}{3} \tan \sigma \ d(v^3)/d\sigma = -g \cos \phi, \quad \xi = ve^{i\phi} \ ,$$

where the sign is determined by inspection.

We will now express Eq. D19 in terms of our basic unknown function $\Omega(t,C)$. Writing

(D20) $$\Omega(t,C) = \tau(t,C) + i\theta(t,C),$$

or $\Omega = \tau + i\theta$, and comparing with Eq. D9, we get the following identities on $t = e^{i\sigma}$ in the quadrant $0 < \sigma < \pi/2$. (Note that, by symmetry, it suffices to satisfy Eq. D19 on this interval.)

$$(1 + t^2) = 2 \cos \sigma \ e^{i\sigma}, \qquad (\cos \sigma > 0),$$

$$(1 - t^2) = 2 \sin \sigma \ e^{i(\sigma - \pi/2)}, \quad (\sin \sigma > 0).$$

Hence, introducing the convenient abbreviation

(D21a) $$L(\sigma) = -\mathrm{Ln}\ (2C \sin \sigma), \quad 0 < 2C < 1,$$

we get by complex trigonometry

$$-\ln C(1-t^2) = \sqrt{M(\sigma)}\, e^{i \arctan\left[(\pi/2-\sigma)/L(\sigma)\right]},$$

where

(D21b) $$M(\sigma) = L^2(\sigma) + \left(\frac{\pi}{2} - \sigma\right)^2 .$$

Since $e^{\Omega} = e^{\tau} e^{i\theta}$ and $\zeta = ve^{i\phi}$, equating absolute values and arguments in Eq. D9, we get

(D22a) $$v = 2|\cos\sigma| \cdot \sqrt[6]{M(\sigma)}\, e^{\tau}, \text{ and}$$

(D22b) $$\phi = \theta + P(\sigma), \text{ where}$$

(D21c) $$P(\sigma) = \sigma + \frac{1}{3}\arctan\left[\left(\frac{\pi}{2} - \sigma\right)/L(\sigma)\right] .$$

We are now ready to rewrite Eq. D19. On $0 < \sigma < \frac{\pi}{2}$, $v^3 = 2(\cos^3\sigma)\sqrt{M(\sigma)}\, e^{3\tau}$. Hence the left-hand side of Eq. D19 is

(D23a) $$Q(\sigma)e^{3\tau}\left\{-\sin\sigma + \left[N(\sigma) + \tau'(\sigma)\right]\cos\sigma\right\},$$

where

(D21d) $$N(\sigma) = \left[-L(\sigma)\cot\sigma - \left(\frac{\pi}{2} - \sigma\right)\right]/3M(\sigma), \text{ and}$$

(D21e) $$Q(\sigma) = 4\sqrt{M(\sigma)}\sin 2\sigma .$$

Similarly, the right-hand side is

(D23b) $$-g\cos\left[\theta + P(\sigma)\right], \quad \text{where } g = \frac{8}{3}e^{3\tau(0)}.$$

The free boundary condition D19 asserts that the functions D23a and D23b are equal.

In terms of the single unknown function $\lambda(\sigma) = \tau'(\sigma)$, we can express $\tau(\sigma) = \underset{\sim}{J}\lambda(\sigma)$ and $\theta(\sigma) = \underset{\sim}{D}\lambda(\sigma)$ by means of singular linear operators $\underset{\sim}{J}$ and $\underset{\sim}{D}$. Hence we can rewrite Eq. D19 as the non-linear integral equation

$$(D24) \qquad Q(\sigma)e^{3\underset{\sim}{J}\lambda}\left\{-\sin\sigma + [N(\sigma) + \lambda(\sigma)]\cos\sigma\right\}$$

$$= -g\cos(\underset{\sim}{D}\lambda + P(\sigma), \quad \text{on } 0 < \sigma < \frac{\pi}{2}.$$

We shall not pursue this further here.

## 8. Discrete Equations.

Instead, we shall use the series expansions

$$(D25a) \qquad \tau(\sigma) = a_2\cos 2\sigma + a_4\cos 4\sigma + a_6\cos 6\sigma + \ldots$$

$$(D25b) \qquad \tau'(\sigma) = -2a_2\sin 2\sigma - 4a_4\sin 4\sigma - \ldots$$

$$(D25c) \qquad \theta(\sigma) = a_2\sin 2\sigma + a_4\sin 4\sigma + a_6\sin 6\sigma + \ldots.$$

The identity between Eqs. D23a and D23b can also be expressed in terms of the coefficients $a_{2k}$, for any given C, by direct substitution. For every $\sigma$, $0 < \sigma < \pi/2$, this gives an equation in the $a_{2k}$.

At the bubble vertex $\sigma = 0$, Eq. D19 becomes singular. Hence we replace it by the differentiated form of the equivalent equation

$$v^2 \sin\sigma \, (dv/d\sigma) = -g \cos\phi \cos\sigma \, .$$

Near $t = i$, the curvature $K = d\phi/ds$ satisfies $dv^2 = gKds^2$. Hence, at $t = i$

$$(dv/ds)^2/(ds/d\sigma)^2 = (dv/ds)^2 = gd\phi/ds = g(d\phi/d\sigma)/(ds/d\sigma).$$

Simplifying, we get by Eq. D12,

(D26) $$(dv/d\sigma)^2 = G(d\phi/d\sigma)(ds/d\sigma) = gB(d\phi/d\sigma).$$

But by Eq. D22a, since $\cos(\pi/2) = 0$, we have

(D26a) $$\frac{dv}{d\sigma} = 2\left[L(\frac{\pi}{2})\right]^{1/3} e^{\tau(\pi/2)} = 2\left[-Ln(2C)\right]^{1/3} e^{-a_2+a_4-\cdots}.$$

Similarly, by Eq. D22b,

(D26b) $$\frac{d\phi}{d\sigma} = \theta'(\frac{\pi}{2}) + 1 - \frac{1}{3L(\frac{\pi}{2})}$$

$$= \sum_{p=1}^{\infty} (-)^p \, 2pa_{2p} + 1 + \frac{1}{3Ln(2C)} \, .$$

Substituting from Eqs. D26a and D26b into Eq. D26, we get an equation on the $a_{2k}$ corresponding to the "free boundary" condition at the vertex, $\sigma = \pi/2$.

Since $R/D = ds/D\, d\phi = (ds/D\, d\sigma)/(d\phi/d\sigma)$, and $ds/d\sigma = |dz/dt| = B$ (cf. Eq. D12), we also get from Eq. D26b the relation

(D26c) $$\frac{R}{D} = \frac{B}{D}\left[1 - 2a_2 + 4a_4 - \cdots + \frac{1}{3(\mathrm{Ln}\ 2C)}\right],$$

where $$\frac{B}{D} = \frac{1}{2\pi}\left[\frac{-\mathrm{Ln}\ C}{-\mathrm{Ln}\ 2C}\right]^{1/3} e^{a_2 - a_4 + \cdots},$$

by Eqs. D14b and D14d.

9. Approximate Solution.

We have tried to solve for the $a_{2k}$ approximately by truncation and interpolation. For any n, the free boundary conditions D26, D26a, and D26b at $\sigma_1 = \pi/2$, combined with Eqs. D23a and D23b with Eqs. D25a and D25c at $\sigma = \sigma_2, \ldots, \sigma_n$ give a system of n transcendental equations in the n unknowns $a_2, a_4, \ldots, a_{2n}$, which one can try to solve.

Mr. James Howland, at our suggestion, tried this scheme first for n = 1. He showed that no solution was possible. That is, the equation

(D27) $$3\left[-\mathrm{Ln}(2C)\right] e^{-6a_2} = 1 + \left[3\ \mathrm{Ln}(2C)\right]^{-1} - 2a_2$$

has no real solution $a_2$, for $0 < C < 0.5$.

The next simplest case n = 2, with $\sigma_1 = \pi/2$ and $\sigma_2 = \pi/4$, gives the two equations

(D28a) $$3\left[-\mathrm{Ln}(2C)\right] e^{-6a_2} = 1 + \frac{1}{3\ \mathrm{Ln}(2C)} - 2a_2 + 4a_4,$$

and

(D28b) $$Ke^{-3a_2-6a_4}\left[H + 2a_2\right] = \cos\phi,$$

where $$K = (3\sqrt{2}/4)\left[(-\mathrm{Ln}\,\sqrt{2C})^2 + \pi^2/16\right]^{1/2},$$

$$H = 1 + \left[-\mathrm{Ln}(\sqrt{2}C) + (\pi/4)\right]/3\left[\mathrm{Ln}^2(\sqrt{2}C) + \pi^2/16\right],$$

$$\phi = \frac{\pi}{4} + \frac{1}{3}\arctan\left[\frac{\pi}{-2\ \mathrm{Ln}(2C^2)}\right] + a_2.$$

Note that Eq. D28a can be easily solved for $a_4$, given $a_2$, and then the error in Eq. D28b quickly estimated. By extrapolation and interpolation, a value of $a_2$ making this error negligible can soon be found, for any given C, $0 < C < 0.5$.

This procedure was followed, and the following numerical values were obtained

| C | $a_2$ | $a_4$ | $u_o/\sqrt{gD}$ | R/D |
|---|---|---|---|---|
| 0.125 | 0.1891 | 0.2390 | 0.260 | 0.130 |
| 0.250 | 0.0965 | 0.2098 | 0.255 | 0.153 |
| 0.375 | 0.09965 | 0.2082 | 0.214 | 0.452 |

The values of $u_o/\sqrt{gD}$ so obtained are very consistent, but R/D is much less so, especially for C = 0.375. This fact may be explained by the discussion of Sec. 6; it would seem that the choice C = 1/2e is not far from the "best" value.

Note that the values of $a_4$ are larger than those of $a_2$. This

explains why the case n = 1 did not work. Furthermore, a study of the basic equation D23a = D23b, evaluated in terms of the $a_{2k}$, suggests that the $a_{4k}$ will generally be larger than the $a_{4k+2}$. This suggests that, if the preceding truncation-interpolation method is to be carried further, the next case to try might be n = 4, with $\sigma_1 = 90^\circ$, $\sigma_2 = 65^\circ$, $\sigma_3 = 40^\circ$, $\sigma_4 = 15_o$, and C = 1/2e.

## 10. More Accurate Solutions.

When the number n of interpolation points is large, it is desirable to use an iterative scheme which can be carried out by a digital computer. Two such methods have been investigated using the IBM 701 computer at Los Alamos.

The first was a gradient method. The equations derived in Sec. 8 for the coefficients $a_o, \ldots, a_{2n}$ were written in the form

$$(D29) \qquad F_j(a_o, \ldots, a_{2n}) = 0 \qquad j = 0, \ldots, n$$

corresponding to the n + 1 points $\sigma_j = j\pi/2n$. Setting

$$F = \sum_{j=0}^{n} F_j^2$$

$$\nabla_j F = \partial F/\partial a_{2j}$$

$$|\nabla F|^2 = \sum_{j=0}^{n} (\nabla_j F)^2,$$

the scheme was to add the increment

$$\delta a_j = -\lambda(\nabla_j F)\, F/|\nabla F|^2, \qquad 0 < \lambda \leqq 1$$

to each $a_j$ in order to find the succeeding coefficients. Preliminary calculations with this method using $n = 4$ and $n = 10$ did not seem to converge accurately.

We considered replacing the preceding gradient method by a more accurate method of steepest descent*, but the rate of convergence was too slow for the calculation to be practical on the IBM 701.

Our second method applies directly to the exact problem, and has an infinite variety of possible approximate discretizations. Stated for the exact (continuous) case, let $\theta(\sigma)$ be a trial value for the imaginary part of $-\Omega$ on the boundary. Then the corresponding real part $\tau(\sigma)$ is provided by the pressure condition by integrating Eq. D19 to give

$$v = 3g\int_{\sigma}^{\pi/2} \cot\sigma \cos\phi \, d\sigma \tag{D30}$$

where $\phi$ is determined by $\theta$ through Eq. D22b. Using Eq. D22a, $\tau$ is obtained directly from $v$. Then the iteration is completed by finding the new function $\theta(\sigma)$ by the transformation

---

*A. E. Householder, "Principles of numerical analysis," New York, 1953, p. 132.

$$\theta(\sigma) = \frac{2}{\pi} \sin 2\sigma \int_0^{\pi/2} \frac{\tau(\rho)\, d\rho}{\cos 2\rho - \cos 2\sigma} \tag{D31}$$

which follows from the fact that $\tau(\sigma) + i\theta(\sigma)$ is the boundary value of an analytic function $\Omega$, regular within the unit circle, and satisfying the required symmetry conditions.

Preliminary calculations using this method were carried out using a number of approximate forms of these equations. In most cases the process converged to yield accurate solutions of the approximate equations. However, the results were quite sensitive to the form of approximation, and none of the solutions appeared to converge with decreasing interval size.

To describe these methods, note that Eq. D24 may be written as a differential equation for $\tau$ of the form

$$d\tau/d\sigma = A \cos(\theta + H)\, e^{-3\tau} + B \tag{D32}$$

where A, B, and H are known functions of $\sigma$. Solution of this equation for $\tau$, with the initial condition on $\tau$ at $\sigma = \pi/2$ provided by Eq. D26 is equivalent to using Eqs. D30 and D22a. Although $\sigma = 0$ is a singular point, it turns out that the solutions have a node at $\sigma = 0$, $\tau = \tau_o$, where $\tau_o = \Omega(1)$ is given by the equation preceding Eq. D11.

In the first computation, Eq. D32 was solved for $\tau$, using

the trapezoidal rule difference equations for $n + 1$ equally spaced points. Then the new $\theta$ was found using the formula

$$\text{(D33)} \qquad \theta(\sigma_j) = \frac{2}{n} \sin 2\sigma_j \left\{ \frac{\epsilon_o^j \, \tau(o)}{2\,[1-\cos 2\sigma_j]} + \sum_{k=1}^{n-1} \frac{\epsilon_k^j \, \tau(\sigma_k)}{\cos 2\sigma_k - \cos 2\sigma_j} - \frac{\epsilon_n^j \, \tau(\frac{\pi}{2})}{2[1+\cos 2\sigma_j]} \right\}$$

where

$$\sigma_j = j\pi/2n$$

$$\epsilon_k^j = \begin{cases} 0 & \text{when } j - k \text{ is even} \\ 1 & \text{when } j - k \text{ is odd} \end{cases}$$

This transformation corresponds to the interpolation formulae

$$\tau(\sigma_j) = \sum_{k=o}^{n} a_{2k} \cos 2k\sigma_j$$

$$\theta(\sigma_j) = \sum_{k=o}^{n} a_{2k} \sin 2k\sigma_j .$$

The results for $u_o / \sqrt{gD}$ were:

| | C = .25 | C = .125 |
|---|---|---|
| n = 25 | .2382 | .2404 |
| n = 51 | .2463 | .2485 |
| | | |

The inconsistency of these results seemed to arise chiefly from the singular behavior of the function $\tau(\sigma)$ near $\sigma = 0$, where the solutions of Eq. D32 apparently behave like

$$\tau \sim \tau(o) + \text{const.}/\log \sigma \tag{D34}$$

Even if the numerical integration of Eq. D32 were accurate, the transformation (D33) is bound to be a poor approximation to (D31). This is evidenced in the calculation by a marked oscillation in the successive values of $\theta$ near $\sigma = 0$, which grows worse with increasing $n$.

To test whether an artificial smoothing of $\tau$ would give more reasonable results, the procedure was modified by replacing the first three values $\tau(o)$, $\tau(\sigma_1)$, and $\tau(\sigma_2)$ by the values of a quadratic function with vanishing slope at $\sigma = 0$, which coincides with $\tau$ at $\sigma_3$ in value and slope. As a result, smooth values of $\theta$ were obtained. The values of $u_o/\sqrt{gD}$ were

| | C = .25 | C = .125 |
|---|---|---|
| n = 25 | .2244 | .2269 |
| n = 51 | .2239 | .2261 |

However the convergence of the iterative procedure was very slow, especially for larger $n$. There is evidence of convergence with increasing $n$, at least near the bubble tip, but the method of smoothing seems to make the results depend on the choice of C.

In view of the sensitivity of the solution to the numerical method used, the internal consistency of the last results may not imply an equal absolute accuracy. This is borne out by a comparison with the results of the third calculation, which uses an apparently more rational treatment of the singularity at $\sigma = 0$ than the ad hoc smoothing of the second method.

Consider the functions

$$x = \mathrm{Re}\left\{1/L(\sigma)\right\} \qquad U = \mathrm{Im}\left\{1/L(\sigma)\right\}$$
$$y = \mathrm{Re}\left\{1/L^2(\sigma)\right\} \qquad V = \mathrm{Im}\left\{1/L^2(\sigma)\right\}$$

Since the behavior of $\tau$ near $\sigma = 0$ is expected to have the form (D34), and since $x \sim 1/\log\sigma$ near $\sigma = 0$, the integration of Eq. D32 was carried out using the trapezoidal rule with respect to the variable $x$ rather than $\sigma$, although the points were kept equally spaced in $\sigma$. Then a fit was made to the values of $\tau$ at $\sigma = 0$, $\sigma_1$, $\sigma_2$, in the form of a linear combination

$$\tau_o = a + bx + cy.$$

Thus the function

$$\tau_1 = \tau - \tau_o$$

was smooth at $\sigma = 0$, and its transform $\theta_1$ by (D33) was also smooth. Thus $\theta$ was found from the equation

$$\theta = \theta_1 + \theta_o$$

where

$$\theta_o = bU + cV$$

The results gave better agreement for different values of C, but were unsatisfactory as regards convergence with increasing n. For $n = 25$ we found

| | $C = .25$ | $C = .125$ |
|---|---|---|
| $u_o/\sqrt{gD}$ = | .2238 | .2249 |

But as n increased, the value of $u_o/\sqrt{gD}$ decreased until the procedure failed to converge to a solution for some n between 30 and 50. For $C = .25$, we found

| | $n = 24$ | $n = 30$ | $n = 50$ |
|---|---|---|---|
| $u_o/\sqrt{gD}$ = | .2218 | .2151 | no solution |

To achieve a convincingly accurate solution in future calculations it will probably be necessary to have a better knowledge of the singularity at $\sigma = 0$, not only in the solution of Eq. D30 but also in the transformation (D31). Meanwhile, the results of these preliminary calculations indicate the value $.225 \pm .005$ for $u_o/\sqrt{gD}$.

11. Experimental Results.

Measurements of air bubbles rising through water in vertical tubes have been performed by Russell Duff at this laboratory. The tubes were closed at the top, and water was allowed to fall freely from the bottom. The bubble rise was photographed by an Eastman High Speed Camera operated at a calibrated frame rate.

The first tube (Tube A) was rectangular in cross section, with width $D = 4.0625"$ and thickness $T = 1"$. The second tube (Tube B) had a circular cross section with diameter $D = 4.0625"$.

The bubble vertex height was plotted against time; the plotted points fell on a nearly straight line as long as the bubble was well removed from the tube ends. The slope of this line was taken as the bubble rise velocity $u_o$. Again, the bubble tip radius of curvature $R$ was estimated by making a least squares parabolic fit to a set of four measured points on the bubble surface, 0.6" or less below the bubble vertex. These radii of curvature were averaged over 8 to 10 successive frames. The resulting values were

| | $u_o/\sqrt{gD}$ | R/D |
|---|---|---|
| Rectangular Tube | 0.29 | 0.26 |
| Circular Tube | 0.35 | 0.35 |

It is interesting to compare the experimental data for the rectangular tube with the theoretical predictions for ideal plane

flow summarized in Sec. 10. Evidently, the measured value $u_o/\sqrt{gD} = 0.29$ is nearly 1.3 times the theoretical value of 0.225. Since surface tension and viscosity tend to diminish $u_o$, this discrepancy is probably due to the three-dimensional character of the flow. It is somewhat surprising the $T/D \simeq 1/4$ should reduce $u_o/\sqrt{gD}$ only half-way from the circular case to the case of a slit, but of course $u_o/\sqrt{gD}$ should be larger for a square than a circle. It would be interesting to experiment with tubes with other T,D.

It is also interesting to compare the experimental data for the circular tube with the mean of previous experimental data summarized in Eq. (19), p. 34 of LA-1862. Evidently, the value $R/D = 0.35$ agrees with that deduced from previous experiments, while the value $u_o/\sqrt{gD} = 0.35$ is about 10% higher than the mean of previous values.

## APPENDIX E

## REMARKS ON LAYZER'S MODEL

We start with the velocity fields

$$\text{(E1)} \qquad \dot{z} = \dot{q}\, e^{-z}\, J_o(r), \qquad \dot{r} = \dot{q}\, e^{-z}\, J_1(r) \qquad [0 \leqq r \leqq \beta_1]$$

in the axially symmetric case, and

$$\text{(E1a)} \qquad x = \dot{q}\, e^{-y} \sin x, \qquad y = \dot{q}\, e^{-y} \cos x,$$

in the plane case. These correspond to velocity potentials of the form $-U = \dot{q}\, e^{-z}\, J_o(r)$ and $-U = \dot{q}\, e^{-y} \cos x$, respectively.

From Eq. E1a, $dy/dx = \cot x$, whence $dy = d(\sin x)/(\sin x)$ and the streamlines are

$$\text{(E2a)} \qquad y - K = \text{Ln}(\sin x) \quad \text{or} \quad e^{y} = C \sin x.$$

Similarly, from Eq. E1, $dr/dz = J_1(r)/J_o(r)$. Transposing, and writing $J_o = J_1' + J_1/r$, we get

$$\text{(E2)} \qquad z - K = \text{Ln}\left[r\, J_1(r)\right], \quad \text{or} \quad e^{z} = Cr\, J_1(r).$$

We can now get a parametric expression for the interface. From Eqs. E1a and E2a, $dx/dq = 1/C$, so $x = x_o + (q/C)$. Hence

$d(e^y)/dq = \cos x = \cos (x_o + q/C)$, or $e^y = e^{y_o} + C \sin (x_o + q/C)$.
If the interface is at $y = 0$ for $q = 0$, this gives

(E3a) $$x = a + q \sin a, \quad e^y = [1 + (\sin x)/(\sin a)] .$$

On the wall $x = \pi$, $-d(e^y) = dq$; hence as $q$ increases from 0 to 1, $y$ decreases from 0 to $-\infty$. On the axis $x = 0$, $d(e^y) = dq$; hence the corresponding change in $e^y$ is +1, and $y$ increases from 0 to Ln 2 = 0.693 on the axis, when the interface reaches $y = -\infty$ on the wall; relative amplitude at blow-up is only $0.693/2\pi \simeq 0.11$! In the axially symmetric case Eq. E2, $d(e^y) = J_o(\beta_1)dq = -0.4028\ dq$ on the wall, and increases from 0 to $\text{Ln}\,[1 + (.4028)^{-1}] \simeq 1.25$; the relative amplitude at blow-up is about 0.2

In Stage (1), the term $\nabla U \cdot \nabla U$ is neglected in Bernoulli's pressure equation; hence the pressure field associated with Eq. E1 satisfies

$$\rho(\partial U/\partial t + gy) + p = \text{const.},$$

where $\partial U/\partial t = -\ddot{q}\, e^{-z} J_o(r)$, and $z = q\, J_o(r)$ on the interface. The condition of constant pressure on the interface is therefore $\ddot{q} + gq = 0$, in our dimensionless coordinates. Similarly, in the plane, $\partial U/\partial t = -\ddot{q}\, e^{-y} \cos x$, and $y = q\, e^{-y} \cos x$. Hence, when $\lambda = 2\pi$ and $k = 1$, the condition of constant interface pressure is $\ddot{q} + g k q = 0$, which coincides with the result of Eqs. 12 and 12' of LA-1862, for $a = \rho' = T = 0$.

To calculate the curvature at the bubble vertex, we use the stream functions

$$\psi = r\, e^{-z}\, J_1(r) - r^2/2, \tag{E4}$$

$$\psi = e^{-y} \sin x - x = x\left[(1 - y + \ldots)(1 - x^2/6 + \ldots) - 1\right] \tag{E4a}$$

which are easily deduced from Layzer's formulas, by superposing a unit velocity along the axis, so as to get steady flow with a stagnation point at (0,0). The corresponding streamlines $\psi = 0$ through (0,0) satisfy the equations, obtained by factoring out $r$ and $x$ in Eqs. E4 and E4a,

$$e^{-z} = r/2J_1(r) = 2/(r - r^3/8 + \ldots), \tag{E5}$$

or $\quad 1 - z + \ldots = 1 + r^2/8 + \ldots,$ and

$$0 = -y - x^2/6 + \ldots \tag{E5a}$$

This gives radii of curvature $R = 4$ and $R = 3$, respectively, in the two cases, where $d = 2\beta_1$ and $d = 2\pi = \lambda$.

## APPENDIX F

## CALCULATION OF INTERFACE MOTION*

### 1. Periodic Vortex Layers.

We shall consider below the two-dimensional Helmholtz and Taylor instability of a periodic interface, separating two ideal fluids of densities $\rho$ and $\rho'$. If $V(x,y;t)$ and $V'(x,y;t)$ are the stream functions describing the motions of the two fluids, then the combined potential $(V,V')$ is the potential of a single layer $\mu$ on the interface $S$ separating the fluids, just as in Appendix B, Sec. 2. Hydrodynamically, $\mu$ is a "vortex layer" for the velocity field whose potential $(U,U')$ is conjugate to $(V,V')$.

The aim of this appendix is to show how the vortex density per unit length $\gamma = 2\, d\mu/ds$, and the geometry of the (periodic) interface, can be taken as dependent variables, so as to calculate effectively the evolution of an interface of arbitrary initial shape.

Specifically, we let the real independent variable $a$ refer to a "material point" on $S$; we let $z(a,t) = x(a,t) + i\, y(a,t)$ denote

*Written jointly with David Carter. James Howland also assisted in the preparation of this appendix, and we have profited from discussions with John Wheeler.

its complex position in the physical plane at time $t$; and we let $\omega$ denote the (periodic) vorticity density in terms of $a$, so that $2d\mu = \omega(a,t)\,da$. For simplicity, we normalize units so that

(F1) $$\omega(a+1) = \omega(a), \qquad z(a+1) = z(a) + \pi.$$

Thus any interval $\alpha \leqq a < \alpha + 1$ constitutes a "complete period," and we use the symbol $\oint$ to denote integration over a complete period.

If the velocities of infinity in $R$ and $R'$ are equal and opposite, the complex potential $(W,W')$ is then defined at any point $z_1$ of $R$ or $R'$ by

(F2) $$W(z_1,t) = \frac{i}{2\pi}\oint \operatorname{Ln}\sin\big(z_1 - z(a,t)\big)\,\omega(a,t)\,da.$$

Conversely, any continuous $\omega(a,t)$ and $z(a,t)$ define a <u>kinematically</u> possible flow, whose normal velocity-component $\partial U/\partial n = \partial U'/\partial n$ is continuous across $S$: $z = z(a,t)$. The tangential component of velocity has a jump of $\gamma(a) = \omega(a)/|\partial z/\partial a| = 2\mu'(a)$ across $S$.

In the case of zero velocity at infinity (pure Taylor instability), $\oint \omega(a,t)\,da = 0$; this is the case in which we are primarily interested. In the general case, $\oint \omega(a,t)\,da \neq 0$, it is convenient to superpose a constant translation velocity on the whole system (i.e., to use moving axes), so that the relation $\rho u_\infty + \rho' u'_\infty = 0$ is satisfied.

We define the velocity of a point $z(a,t)$ on the vortex layer itself as the complex conjugate of the Cauchy <u>principal value</u> of the

(divergent) integral

$$\dot{z}^*(a,t) = \frac{i}{2\pi} \oint \cot\big(z - z(a',t)\big)\, \omega(a',t)\, da'. \tag{F3}$$

This velocity $\dot{z}(a,t)$ is the average of the vector velocities on the two sides. The velocity component normal to S towards R is

$$u_n = \dot{x} \cos\theta \pm \dot{y} \sin\theta \tag{F3a}$$

and the tangential component is

$$u_t = \mp \dot{x} \sin\theta + \dot{y} \cos\theta. \tag{F3b}$$

As we have already seen, $u_n = \partial U/\partial n = \partial U'/\partial n$, while $\partial U/\partial s = u_t - (\gamma/2)$, $\partial U'/\partial s = u_t + (\gamma/2)$.

## 2. Continuity of Pressure.

The pressure in R is defined up to a function P(t) of time alone, by Eq. F2 and the Bernoulli equation

$$p + \rho \partial U/\partial t + \frac{1}{2} \rho \nabla U \cdot \nabla U + \rho g y = P(t). \tag{F4}$$

in R. It is defined up to a second function P'(t) in R', by an analogous equation involving p', $\rho'$ and U'. To be compatible with pressure continuity across S (i.e., to be <u>dynamically</u> possible), a flow defined by Eqs. F2 and F3 must therefore satisfy the condition $\partial p/\partial a = \partial p'/\partial a$.

To evaluate $\partial U/\partial t$ in Eq. F4, we compute

$$(F5) \qquad \dot{W}(z_1,t) = \frac{i}{2\pi}\oint \left\{\dot{\omega}\ \mathrm{Ln}\ \sin(z_1 - z) - \omega \dot{z}\ \cot(z_1 - z)\right\} da.$$

This equation holds on both sides of S. If one evaluates $2/(\rho + \rho')$ times the different terms of the equation $\partial p/\partial a = \partial p'/\partial a$ from Eqs. F4, F5 and F2, taking due care concerning continuity as S is approached, one gets

$$(F6) \qquad \dot{\omega}(a,t) - \alpha \oint K(a,a';t)\ \dot{\omega}(a',t)\ da' = \partial E(a,t)/\partial a,$$

where $\alpha = (\rho - \rho')/(\rho + \rho')$,

$$(F6a) \qquad K(a,a') = \frac{1}{\pi}\ \mathrm{Im}\left\{\partial z/\partial a\ \cot\left[z(a,t) - z(a',t)\right]\right\}$$

as in LA-1862, Eqs. (33) - (33a), and

$$(F6b) \qquad E(a,t) = \alpha\left\{\frac{1}{\pi}\oint \omega(a',t)\ \mathrm{Im}\left[\dot{z}(a',t)\ \cot\big(z(a,t) - z(a',t)\big)\right]da' - |\dot{z}|^2 - \tfrac{1}{4}(\omega da/ds)^2 - 2gy\right\}$$

where the Cauchy principal value of the integral is taken. If interfacial tension T is included, then the expression E(a,t) requires an extra term of the form $-2T\ d\theta/(\rho + \rho')\ ds$, where $\theta$ = arc $\partial z/\partial a$ is tangential direction and so $d\theta/ds$ is the curvature.

To derive formulas F6, F6a, and F6b, we express the identity $\partial p/\partial a = \partial p'/\partial a$ in terms of Eq. F4 and its analog in R', and divide by $(\rho + \rho')/2$. Since $\partial P/\partial a = \partial P'/\partial a = 0$ in any case, we need equate only the derivatives of the left side of Eq. F4 and its analog.

To evaluate $\rho\partial^2 U/\partial t\partial a - \rho'\partial^2 U'/\partial t\partial a$, we consider first the term of Eq. F5 involving the factor $\dot{\omega}$. This is the same as in the case $\omega = \dot{z} = 0$ of initial acceleration, already treated in Appendix B; thus it gives the left side of Eq. F6.

When $\partial U/\partial t = \mathrm{Re}\left\{\dot{W}\right\}$ and $\partial U'/\partial t = \mathrm{Re}\left\{\dot{W}'\right\}$ are evaluated by Eq. F5, the terms in $\dot{z}^*$ contribute the first term on the right side of Eq. F6b, partially expressing $(\rho\partial U/\partial t - \rho'\partial U'/\partial t)/2(\rho + \rho')$.

The term in $G = gy$ also occurs in the case of initial acceleration, and gives the term $2\alpha gy$ in Eq. F6b.

The evaluation of $\frac{1}{2}\rho\nabla U\cdot\nabla U - \frac{1}{2}\rho'\ \nabla U'\cdot\nabla U'$ is immediate from Eqs. F3a and F3b. Indeed,

$$\nabla U\cdot\nabla U = u_n^2 + u_t^2 - \gamma u_t + \gamma^2/4$$

$$\nabla U'\cdot\nabla U' = u_n^2 + u_t^2 + \gamma u_t + \gamma^2/4$$

The last term gives the contribution $-\alpha\gamma^2/8$. The first two terms give $\alpha\left|\dot{z}^2\right|/2$, where $\dot{z}$ is given by Eq. F3. The third term gives $-\gamma u_t/2$.

Finally, the surface tension makes the obvious contribution of $-2(\rho + \rho')^{-1}\ T\ d\theta/ds$, where $d\theta/ds$ is the curvature.

## 3. Physical Discussion.

It is interesting to give a physical interpretation to the various terms of Eqs. F6, F6a, and F6b, in terms of the idea that S is a

continuum of material vortex-points.

We first show that $\dot{z}(a,t)$ gives the limiting convection of the boundary layer separating R and R', as the viscosities $\mu$, $\mu'$ tend to zero -- regardless of their ratio. We consider the special case of parallel motion and a straight interface, on the assumption that normal motion and curvature do not affect the local boundary layer behavior. In this case, the vorticity $\gamma$ per unit length is given by

$$\gamma = \int u_y \, dy = u_2 - u_1, \tag{F7}$$

the jump in tangential velocity across the boundary layer. The rate of tangential convection of vorticity is

$$\int u \, u_y \, dy = \frac{1}{2} (u_2^2 - u_1^2). \tag{F7'}$$

Hence the effective tangential velocity is the mean velocity $\frac{1}{2} (u_2 + u_1)$, as given by Eq. F3.

We next show that, in the absence of surface tension, the rate of change of vorticity over a section of S is given by

$$2 \int_a^b d\mu = g(\rho - \rho')\big(z(b) - z(a)\big). \tag{F8}$$

To see this, we suppose the viscosity zero, but suppose a thin boundary layer as in the preceding paragraph. We then apply the classic Helmholtz-Kelvin formula for the rate of change of circulation

$$\Gamma = \oint \frac{d\vec{x}}{dt} \cdot \frac{\partial \vec{x}}{\partial a} \, da = \int \vec{u} \, d\vec{x}$$

around a closed curve. We use Lagrangian coordinates, but let $d/dt = (\partial/\partial t)_a$ denote material differentiation. Then

$$\frac{d\Gamma}{dt} = \oint \frac{d\vec{u}}{dt} \cdot \frac{\partial \vec{x}}{\partial a}\, da + \oint \vec{u}\, \frac{\partial^2 x}{\partial a \partial t}\, da.$$

But $\partial^2 x/\partial a \partial t = \partial \vec{u}/\partial a$, hence the second term is $\oint \vec{u} \cdot d\vec{u} = 0$. Since $d\vec{u}/dt = \nabla p/\rho + g$, the first term is

$$\oint \frac{1}{\rho}\, \nabla p \cdot d\vec{x} + \oint \vec{g} \cdot d\vec{x} = \left(\frac{1}{\rho} - \frac{1}{\rho'}\right) \left[p\big(z(b)\big) - p\big(z(a)\big)\right].$$

That is, in summary,

$$d\Gamma/dt = \left(\frac{1}{\rho} - \frac{1}{\rho'}\right) \left[p\big(z(b)\big) - p\big(z(a)\big)\right]. \tag{F9}$$

Differentiating with respect to a, we get finally

$$\partial \omega/\partial t = \left(\frac{1}{\rho} - \frac{1}{\rho'}\right) \frac{\partial p}{\partial a}. \tag{F9'}$$

To justify the last step, we must show that, in the limit, the convection of the contour of integration does not affect $d\Gamma/dt$. That

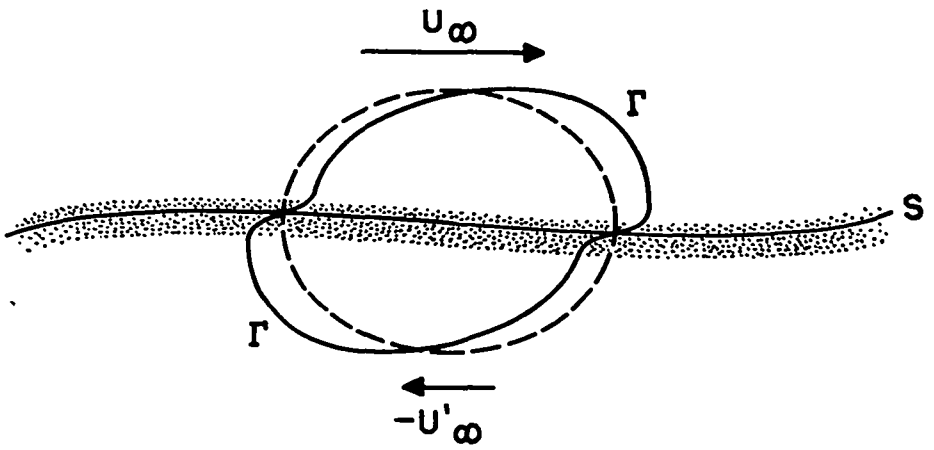


Fig. 1

is, referring to Fig. 1, we must show that the net convection of vorticity is zero. But this is the significance of Eqs. F7 and F7'.

## 4. The Case $\alpha = 0$.

The case $\alpha = 0$ of pure Helmholtz instability greatly simplifies Eq. F6. Indeed, if the surface tension T is neglected, then Eq. F6 or Eq. F9' is equivalent to

$$\omega = \omega(a). \tag{F10}$$

Hence, in this case, the problem is simply to integrate Eq. F3, which we rewrite as

$$\dot{z}(a,t) = \frac{1}{2\pi} \oint \cot\big(z - z(a',t)\big)\omega(a')\, da'. \tag{F10}$$

This problem has been treated numerically by L. Rosenhead* using desk machines, in a well-known paper.

Specifically, assuming a unit vorticity for each of N equal point vortices, and unit relative velocity, we have the system of 2N ordinary differential equations

$$\dot{x}_i = \frac{U}{N} \sum_{k \neq i} \frac{\sinh \pi k(y_i - y_k)/N}{\cos h\, \pi k(y_1 - y_k)/N - \cos \pi k(x_i - x_k)} \tag{F11a}$$

*L. Rosenhead, Proc. Roy. Soc. A134 (1931), 170 - 92. See also E. C. da N. Andrade, Proc. Phys. Soc. London 53 (1941), 329 - 55.

(F11b) $$\dot{y}_i = -\frac{U}{N}\sum_{k\neq i}\frac{\sin\pi k(x_i - x_k)}{\text{same denominator}}\,.$$

(cf. Rosenhead, op. cit., Eq. 13).

This system was integrated numerically by Rosenhead for $N = 8, 12$, using desk machines. He used a secant integration formula, except that when the curvature of $S$ became extreme, he supposed the four vortices nearest the center of maximum vorticity to rotate about that center with constant angular velocity. The curves of the "rolling up of the vortex sheet" so obtained have been frequently reproduced, and are indeed classic.

## 5. Extension of Rosenhead's Analysis.

However, we believe that the usual literal interpretation of these curves represents an oversimplification of the true facts. We shall now present the evidence for this belief.

In our attempt to extend Rosenhead's method, we first repeated the case of 12 vortices per wavelength $\lambda$, with the same initial "perturbation" amplitude of $0.1\,\lambda$, and a sinusoidal interface. With time steps $t \leqslant 0.5\,\lambda/U$, our results were in fair agreement with those of Rosenhead until $t \sim 0.35\,\lambda/U$, when the vortex sheet begins to curl over. Beyond this point, unsmoothed calculations gave an erratic interface.

No improvement in the smoothness was obtained by increasing

the number N of vortices per wavelength, decreasing the time step $\delta t$, or by using a more accurate Runge-Kutta integration scheme. For example, the case N = 48 exhibited the same type of instability with the much smaller initial sinusoidal perturbation $y = 0.01\lambda \sin x$. In fact, with this more nearly infinitesimal initial perturbation, the wave crest began to curl over at an amplitude of $0.1\lambda$ (as contrasted with $0.15\lambda$ in Rosenhead's calculations).

A critical reconsideration of the problem led us to study the relevance of the theoretical observations of LA-1862, p. 50. These are (i) that the evolution of a vortex sheet (or other discontinuity) is probably well-determined mathematically only for a limited interval of time, and (ii) that the calculations can be stabilized by assumimg an interfacial tension.

In order to give these views a careful test, by an otherwise stable numerical calculation, we used the method outlined in Secs. 1 - 2 above, but keeping the vortex centers equally spaced with respect to arc-length along the interface. Figures 2 through 4 show the results for 32 points per wavelength. Each figure shows the development of a half-wavelength, for successive values of t. The vertical scales are expanded by a factor 2 over the horizontal. Distances are measured in units of $1/k = \lambda/2\pi$, and time in units of 1/kU. In all cases the initial perturbation amplitude was $0.01/k \simeq 0.0016\lambda$. Figure 2 is for the case of zero surface tension T = 0, with the expected instability. Figures 3 and 4 are for $kT/2\rho U^2 = 3/32$ and 3/16,

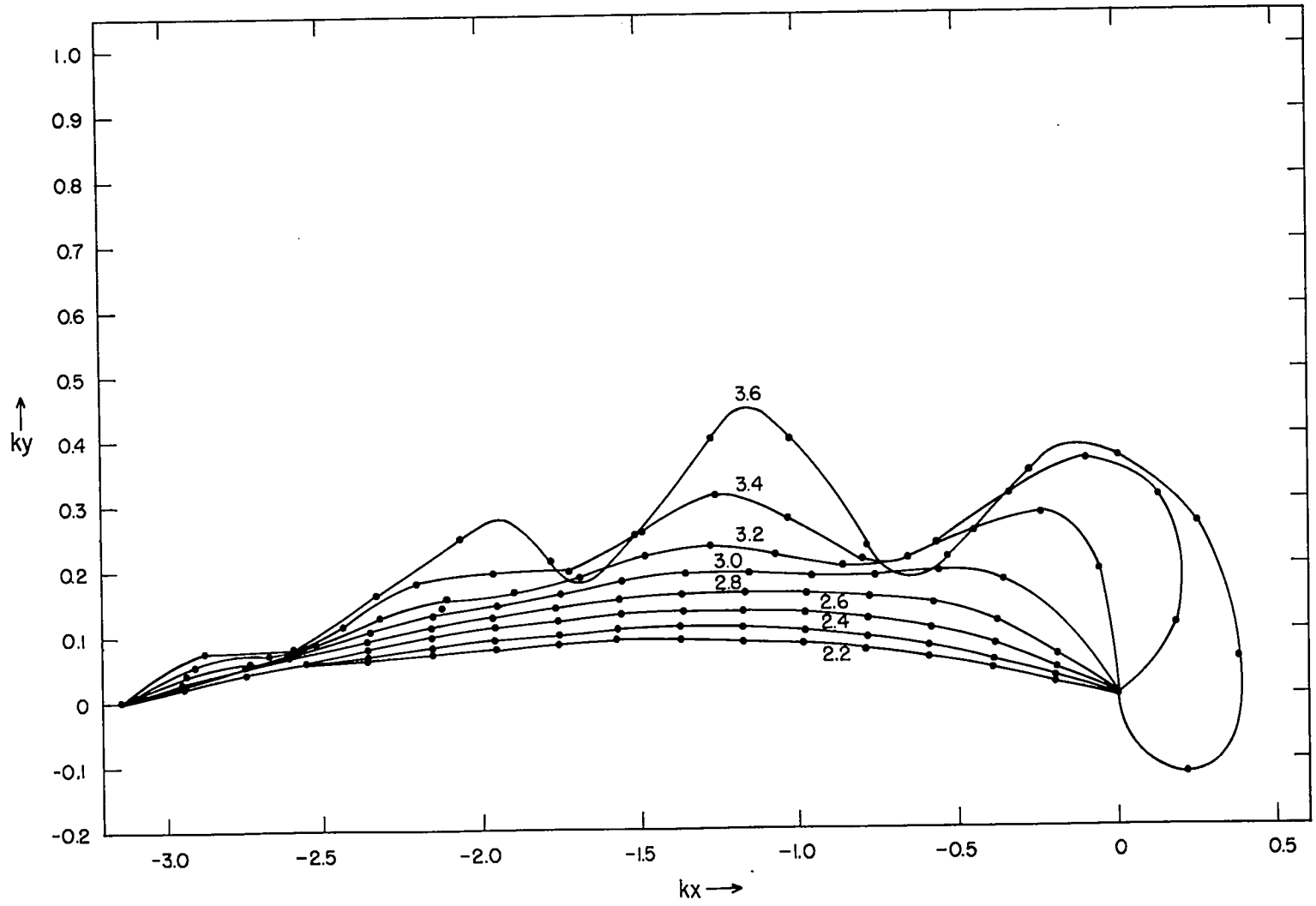


Fig. 2 Progressive interface configurations for T = 0. Numbers on curves are values of kUt.

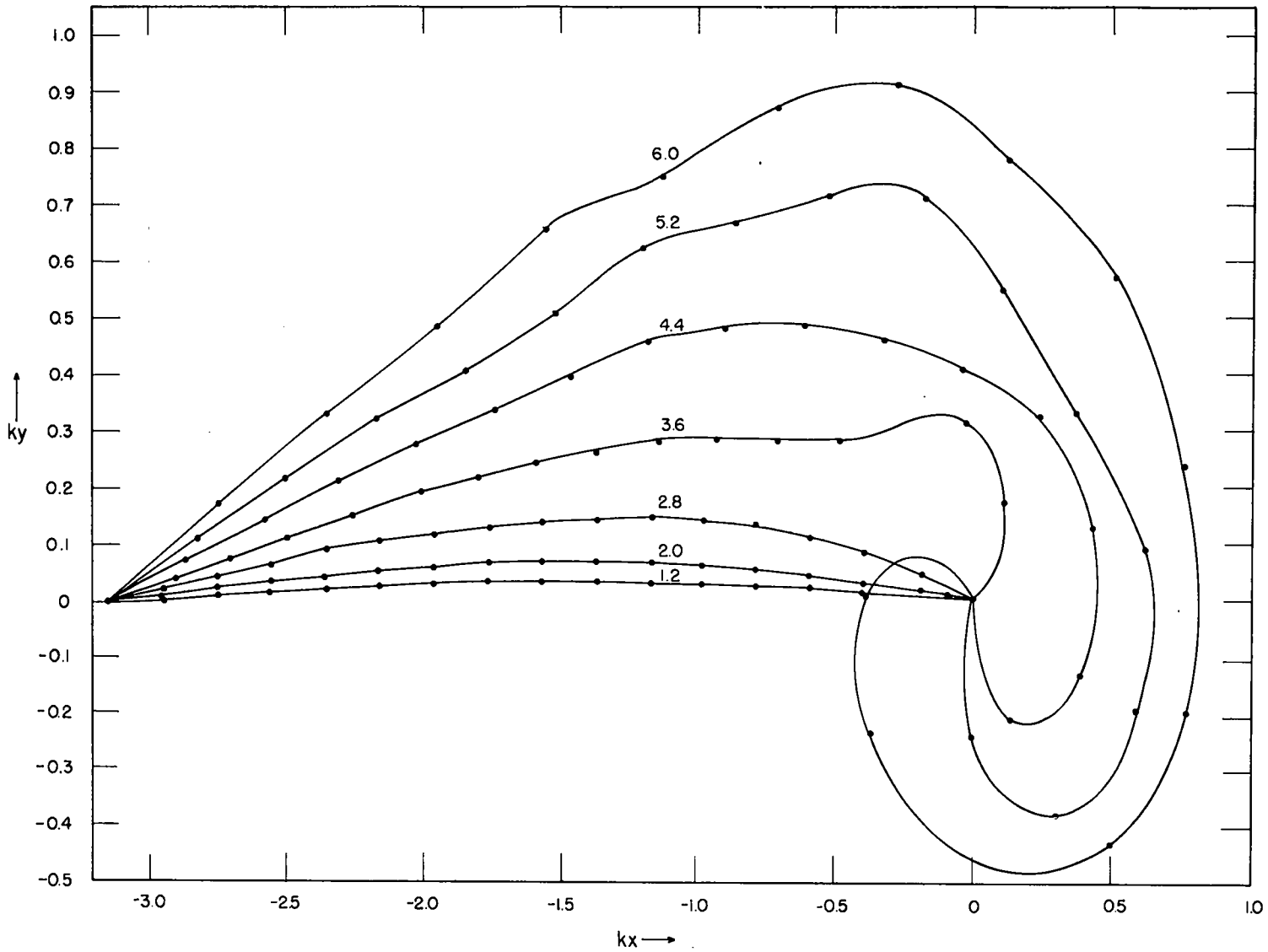


Fig. 3 Progressive interface configurations for $kT/2\rho U^2 = 3/32$. Numbers on the curves are values of kUt.

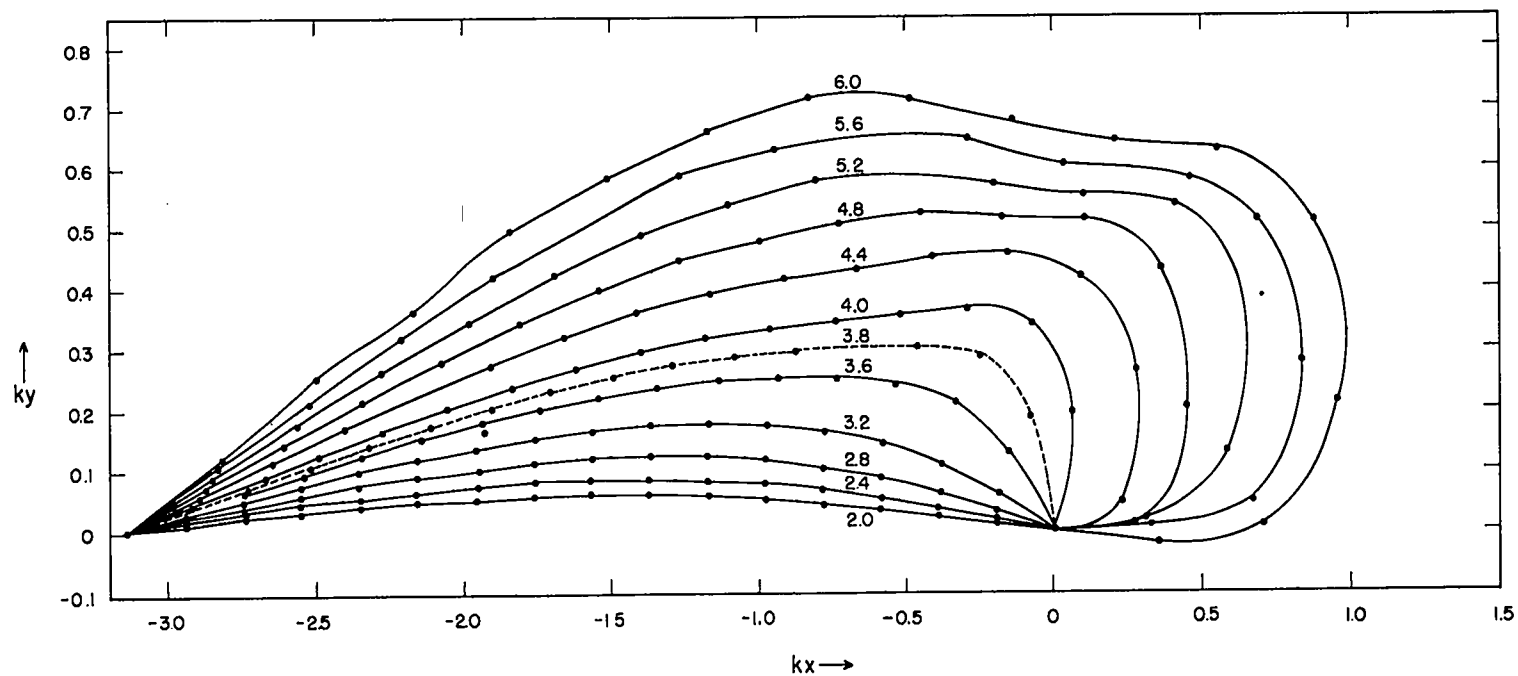


Fig. 4 Progressive interface configurations for $kT/2\rho U^2 = 3/16$. Numbers on the curves are values of kUt.

respectively. In the latter cases, the calculations were stopped when the results had lost their quantitative significance. Although stability required taking a short time step, inversely proportional to the number of points per wavelength, no violent instability occurred with sufficiently short steps.

It should be possible, therefore, to obtain unlimited accuracy for $T > 0$ by taking many points and correspondingly short time steps.

It may be of interest to note that the use of a small number of vortices exercises a stabilizing effect on interface waves, somewhat analogous to that of surface tension. Specifically, the exponential growth factor for an infinitesimal sine wave of wavelength $\lambda/n$, with N vortices, is

$$\alpha = nk\,U\left(1 - \frac{n}{N}\right) = 2\pi\,\frac{U}{\lambda}\,n\left(1 - \frac{n}{N}\right). \tag{F12}$$

Comparing this with the growth factor for the "continuous" case $N = \infty$ with surface tension,

$$\alpha = nk\,U\sqrt{1 - (n\,kT/2\rho U^2)}, \tag{F12'}$$

we see that for the fundamental node $(n = 1)$, the two effects are equal with

$$T = 4\rho U^2/kN(1 - 1/2N). \tag{F13}$$

For $n > 1$, the "effective surface tension" is even more.

The authors wish to thank Professor John Wheeler for discussions of these calculations.

# TAYLOR INSTABILITY OF AN INCOMPRESSIBLE LIQUID

by

Enrico Fermi
September 4, 1951

This is an attempt to discuss in a very simplified form the problem of the growth of an initial ripple on the surface of an incompressible liquid in presence of an acceleration, g, directed from the outside into the liquid.

The model is that of a heavy liquid occupying at $t = 0$ the half space above the plane $z = 0$. It is well known that this is a state of unstable equilibrium. Any tiny ripple on the surface at the initial time grows in amplitude, first exponentially and later, when its amplitude has become comparable to the wavelength, by a more complicated law.

The case will be considered that there is initially a small amplitude sinusoidal ripple of wavelength $\lambda$. In a first phase this amplitude will increase exponentially like

$$\exp\left(\sqrt{\frac{2\pi g}{\lambda}}\, t\right) \tag{1}$$

This exponential law, however, will break down when the amplitude has become comparable to $\lambda\!\!\!^{-} = \lambda/2\pi$. We propose to discuss what happens in the subsequent phase.

This will be done by grossly schematizing the shape of the wave as indicated in Fig. 1.

Instead of a wave profile like the curve, a profile like ABCDEFGHIJ will be assumed.

It is clear from the symmetry of the problem that the points at the maximum and the minimum of the wave move in vertical directions. In Fig. 2 a half wave, from a maximum to the successive minimum is represented with the notations adopted. OO' is the initial level of the liquid. On account of the incompressibility, the amount of liquid below the plane OO', namely CO'DE must be equal to the amount of liquid ABCO missing from above. This condition leads immediately to the relationship

$$b = \frac{ax}{1-x} \tag{2}$$

Our schematic wave profile is then characterized by the two parameters a, x. The problem is to determine how they vary with time.

In principle the problem so simplified could be solved by expressing the kinetic energy T and the potential energy U of the liquid contained between the two boundaries OA, O'E as functions of a, x, $\dot{a}$, $\dot{x}$.

$$T = T(a, x, \dot{a}, \dot{x})$$

$$U = U(a, x)$$

One can then write the Lagrange equations

$$\frac{d}{dt}\frac{\partial T}{\partial \dot{x}} - \frac{\partial T}{\partial x} = -\frac{\partial U}{\partial x}; \quad \frac{d}{dt}\frac{\partial T}{\partial \dot{a}} - \frac{\partial T}{\partial a} = -\frac{\partial U}{\partial a} \tag{3}$$

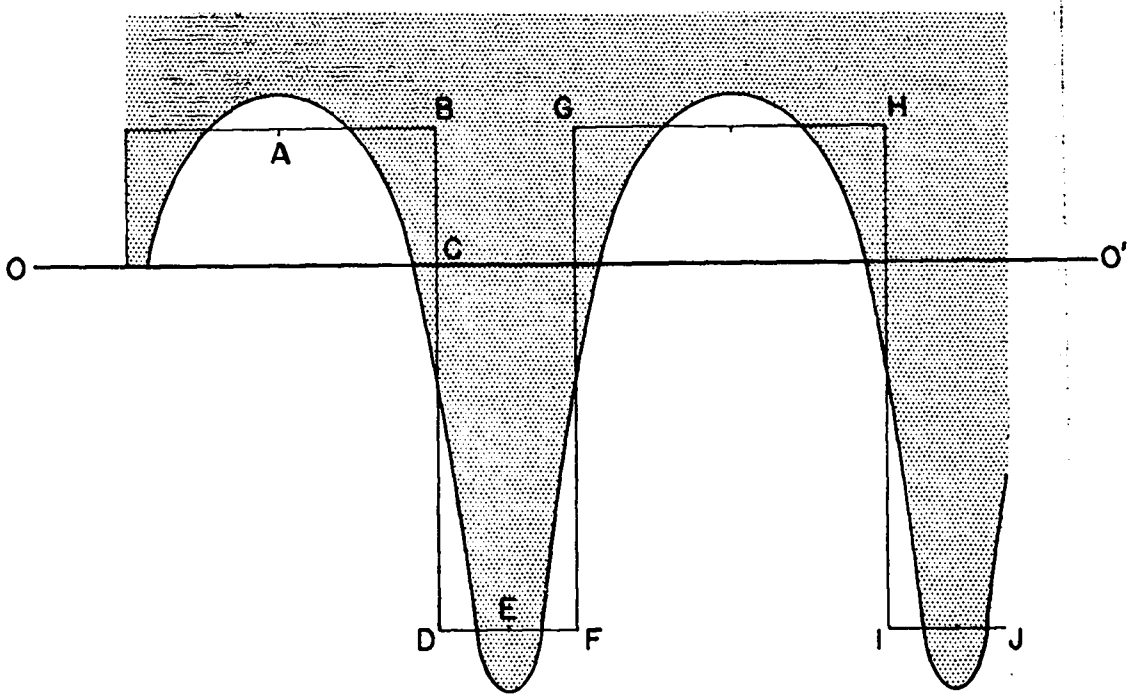


Fig. 1

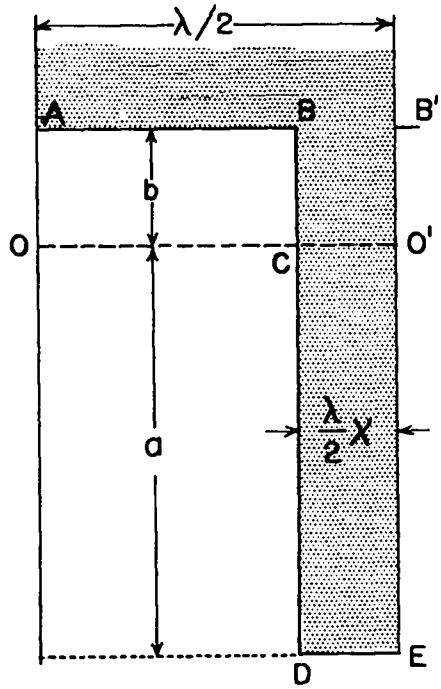


Fig. 2

which describe the law of variation of the two wave parameters $\underline{a}$, $\underline{x}$.

The potential energy U can be written down immediately. It is due to having moved the liquid originally contained in ABOC (weight per unit length perpendicular to the plane of the drawing = $\rho g \frac{\lambda}{2} b(1 - x)$, height of the center of gravity = $b/2$) to the lower position CDEO' with the center of gravity at a height $-a/2$.

In what follows the following unit will be used: unit of length, $\frac{\lambda}{2}$; unit of acceleration, g; unit of density, $\rho$.

One finds, then, the potential energy

$$U = -\frac{1}{2}\frac{a^2 x}{1-x} \tag{4}$$

The calculation of the kinetic energy is more difficult. In principle it could be carried out for a prescribed motion of the profile of the liquid by solving a Dirichlet problem. Instead of doing this, a much cruder method was followed in keeping with the crude approximation chosen for the profile of the wave.

When the amplitude of the wave is very large, it is evident that the kinetic energy is due primarily to the vertical component of the liquid velocity inside the domain BDEB'. The corresponding kinetic energy can be computed easily on the assumption that the vertical component of the velocity is constant on each horizontal section of BDEB'. One finds that this part of the kinetic energy is given by

$$T_1 = \frac{a^3 x^2}{6x(1-x)} \tag{5}$$

For small and moderate amplitudes of the wave, additional terms in the kinetic energy become important. One of them is the kinetic energy due to the horizontal component of the motion of the liquid BDEB'. This term of the kinetic energy is given approximately by

$$T_2 = \frac{a x \dot{x}^2}{6(1-x)} \tag{6}$$

Finally, the kinetic energy due to the motion of the liquid above the line AB' should be estimated. An approximate expression for this term of the kinetic energy yields

$$T_3 = \frac{\pi}{4} \frac{a^2 \dot{x}^2}{(1-x)^2} + \frac{\pi}{2} \frac{a x \dot{a} \dot{x}}{1-x} + \frac{\pi}{4} x^2 \dot{a}^2 \tag{7}$$

The kinetic energy is the sum of the three terms (5), (6), (7)

$$T = T_1 + T_2 + T_3 \tag{8}$$

As pointed out, the leading term at high amplitude is the first. For low amplitude all the three terms need to be considered.

Using the expressions (4) and (8) for potential and kinetic energy, one can write the Lagrange equations (3). That enables one to express the second time derivatives $x$ and $a$ in terms of $x$, $a$, $\dot{x}$, $\dot{a}$. One finds

$$\ddot{x} = \frac{ED-FB}{AB-BC}, \quad \ddot{a} = \frac{AF-EC}{AD-BC} \tag{9}$$

where

$$A = \frac{a^2}{3y} + \frac{y}{3} + \frac{\pi}{2} a, \quad D = a + \frac{\pi}{2} y$$

$$B = \frac{a}{2} + \frac{\pi}{2} y, \qquad C = \frac{a^2}{2y} + \frac{\pi}{2} a \tag{10}$$

$$E = \frac{a}{2} - \frac{\dot{a}^2}{2} - \frac{1}{6}\,\frac{(4x-1)a^2\dot{x}^2}{y^2} - \frac{a\dot{a}\dot{x}}{y} - \frac{\dot{x}^2}{6} - \frac{y\dot{x}\dot{a}}{3a} - \frac{\pi}{2}\,\frac{xy\dot{a}^2}{a} - \frac{\pi}{2}\,\frac{ax\dot{x}^2}{y} - \pi\dot{x}\dot{a}$$

$$F = a - \frac{\dot{a}^2}{2} + \frac{(1-2x)a^2\dot{x}^2}{2y^2} - \frac{a\dot{x}\dot{a}}{y} + \frac{\dot{x}^2}{6} - \pi\frac{y\dot{x}\dot{a}}{x} \qquad (11)$$

and

$$y = x(1-x) \qquad (12)$$

These equations have been integrated numerically by Miriam Caldwell. Initial conditions corresponding to a wave of very low amplitude were chosen as follows: $a = .01$, $\dot{a} = .0177$, $x = .5$, $\dot{x} = 0$. The results of the numerical integration are given in Table I.

| t | a | b | x |
|---|---|---|---|
| 0 | .0100 | .0100 | .500 |
| .5 | .0243 | .0228 | .484 |
| 1.0 | .0628 | .0468 | .427 |
| 1.5 | .192 | .083 | .303 |
| 2.0 | .584 | .115 | .165 |
| 2.5 | 1.218 | .144 | .106 |
| 3.0 | 2.195 | .170 | .072 |

Table I

The four columns of the table give, respectively: the time in units $\sqrt{\frac{\lambda}{2g}}$ ; the two amplitudes of the wave, a and b, below and above the original surface of the liquid expressed in units $\lambda/2$; and the quantity x that measures the asymmetry of the wave ($x = .5$ corresponding to a symmetrical wave). $x < .5$ corresponds to a wave in which the half wave below the original liquid surface is narrower than the half wave above. From an inspection of the table one will recognize that up to about

$t = 1$, the two amplitudes, $\underline{a}$ and $\underline{b}$, have rather close values and they grow approximately exponentially with a period not far from the one computed from the correct hydrodynamical theory of small amplitude waves

$$T = \sqrt{\frac{\lambda}{2\pi g}} = \frac{1}{\sqrt{\pi}} = .56 \quad \text{(in our units)} \tag{13}$$

Already, at $t = 1$, an appreciable asymmetry of the wave has developed. This becomes more and more noticeable for later times. At $t = 3$, for example, $b$ is less than 1/10th of $a$.

The asymptotic behavior of $\underline{a}$, $\underline{b}$, and $\underline{x}$ for large values of the time is obtained from a discussion of equations (9). One finds that $\underline{a}$ increases proportionally to the square of the time, $b$ increases proportionally to the square root of the time, and $x$ is inversely proportional to the $3/2$ power of the time. More precisely, one finds the following limiting expressions

$$a \longrightarrow \frac{4}{7}(t - 1.04)^2 \tag{14}$$

$$b \longrightarrow .12\,(t - 1.04)^{1/2} \tag{15}$$

$$x \longrightarrow .21\,(t - 1.04)^{-3/2} \tag{16}$$

In other words, the lower tip of the wave falls with uniformly accelerated motion and with acceleration equal to $8g/7$. The upper half wave grows much slowly and its velocity decreases with time.

It is interesting to compare the results of this crude approximation with the experimental results obtained by D. J. Lewis,[1] as well as

---

[1] PRS 202A 81, 1950

with the results of G. I. Taylor[2] and of Taylor and Davies.[3] The present theory seems to represent correctly one feature of experimental results, namely the fact that the half wave of the heavy liquid into the vacuum becomes rapidly narrower, whereas the half wave pushing into the heavy liquid becomes more and more blunt. On the other hand, the present theory fails to account for the experimental results according to which the front of the wave pushing into the heavy liquid moves with constant velocity. According to the present theory the displacement is expected instead to be proportional to the square root of the time.

---

[2] PRS 201A 192, 1950

[3] PRS 200A 375, 1950

## APPENDIX G

## MOTION OF POLYGONAL INTERFACE (FERMI MODEL)

### 1. Introduction.

In Secs. 28-29 of LA-1862, a general discussion was given of Fermi's idea that one might approximate actual Taylor instability by constraining the interface to be polygonal. For convenient reference, Fermi's original memorandum is reproduced at the end of Appendix G.

The present appendix is intended to give some formulas which would be useful if calculations were made based on Eqs. 36 through 46 of LA-1862. It was originally intended to make such calculations, but the other two methods described in Part IV of LA-1862 seem more promising.

The formulas given below refer to Sec. 29 of LA-1862, and to the notation used there. They are taken from Ref. 4 of LA-1862, and were derived by R. L. Ingraham and the present author.

### 2. The $\partial x_i/\partial q_\lambda$ and $\partial y_i/\partial q_\lambda$.

The partial derivatives in Eqs. 45a and 45b of LA-1862 can be expressed as definite integrals. In view of Eqs. 44c and 44d, it suffices to evaluate the $\partial \Phi_i/\partial q_\lambda$ and $\partial \ell_i/\partial q_\lambda$.

Again, in view of Eq. 44a, the $\partial \Phi_i/\partial q_\lambda$ are trivial. Clearly, $\partial \Phi_i/\partial \alpha_j = 0$, $\partial \Phi_i/\partial \mu_j = 0$ if $i \leq j$, and $\partial \Phi_i/\partial \mu_j = \pi$ if $i > j$. Therefore, it remains to evaluate the $\partial \ell_i/\partial q_\lambda$. Again,

by Eqs. 44b and 43, we have

$$(G1) \qquad d\ell_i = A\,dI_i + A^2 I_i\,(I_i \sin\Phi_i\, d\Phi_i - \cos\Phi_i\, dI_i).$$

To evaluate the $\partial \ell_i/\partial q_\lambda$, since we know the $\partial \Phi_i/\partial q_\lambda$, it therefore remains to evaluate the $\partial I_i/\partial q_\lambda$. In view of Eq. 42, these are given by the following formulas:

$$(G2a) \qquad \frac{\partial}{\partial \mu_j} I_i = \int_{\alpha_{i-1}}^{\alpha_i} \frac{1}{|R(\xi)|} \ln\left\{\frac{1-\xi}{|\alpha_j - \xi|}\right\} d\xi$$

$$(G2b) \qquad \frac{\partial}{\partial \alpha_j} I_i = -\mu_j \int_{\alpha_{i-1}}^{\alpha_i} \frac{d\xi}{|R(\xi)|(\alpha_j - \xi)} \quad [j \neq i,\ i-1]$$

$$(G2c) \qquad \frac{\partial}{\partial \alpha_i} I_i = -\mu_i \int_{\alpha_{i-1}}^{\alpha} \frac{d\xi}{|R(\xi)|(\alpha_i - \xi)} + \int_{\alpha}^{\alpha_i} (\alpha_i - \xi)^{-\mu_i} S_i'(\xi)\,d\xi + \frac{1}{|R(\alpha)|}$$

$$(G2d) \qquad \frac{\partial}{\partial \alpha_{i-1}} I_i = -\mu_{i-1} \int_{\alpha}^{\alpha_i} \frac{d\xi}{|R(\xi)|(\alpha_{i-1} - \xi)} + \int_{\alpha_{i-1}}^{\alpha} (\xi - \alpha_{i-1})^{-\mu_{i-1}} S_{i-1}'(\xi)\,d\xi - \frac{1}{|R(\alpha)|}.$$

Here $\alpha$ is arbitrary subject to $\alpha_{i-1} < \alpha < \alpha_i$, and

$$(G2e) \qquad S_j(\xi) = \frac{(\xi - \alpha_j)^{\mu_j}}{|R(\xi)|}, \qquad S_j'(\xi) = \frac{d}{d\xi} S_j(\xi).$$

It is not guaranteed that the singularities at $\alpha_i$ have been treated in the preceding formulas, so as to give absolute convergence under the most general circumstances. However, as the $\partial I_i/\partial q_\lambda$ are closely related to the Schläfli determinant, a study of the literature on this* should enable one to get formulas having the most desirable convergence properties.

3. Kinetic Energy Tensor.

On the other hand, some numerical work was done on the effective calculation of the $T_{\kappa\lambda}(\vec{x})$. To calculate the $T_{\kappa\lambda}(\vec{x})$, it is convenient to replace Eq. (46) of LA-1862 by the equivalent formula

$$(G3) \qquad T_{\kappa\lambda} = -\pi^{-1}\left[a_{i\kappa}a_{j\lambda}I^{ij} + (a_{i\kappa}n_{j\lambda} + a_{i\lambda}b_{j\kappa})J^{ij} + b_{i\kappa}b_{j\lambda}\kappa^{ij}\right],$$

where, writing $F(\xi, \xi')$ for $\mathrm{Ln}\,|\xi - \xi'|/|R(\xi)\,R(\xi')|$,

$$(G4a) \qquad I^{ij} = \int_{\alpha_{i-1}}^{\alpha_i}\int_{\alpha_{j-1}}^{\alpha_j} F(\xi, \xi')\,d\xi\,d\xi',$$

$$(G4b) \qquad J^{ij} = \int_{\alpha_{i-1}}^{\alpha_i}\int_{\alpha_{j-1}}^{\alpha_j} s_i\,F(\xi, \xi')\,d\xi\,d\xi',$$

*Phragmen, Acta Math. 14 (1890), p. 230; A. Weinstein, Math. Zeits. 21 (1924), p. 72; J. Kampé de Fériet, Ann. Soc. Sci. Bruxelles 49 (1927), p. 55.

$$(G4c) \qquad \kappa^{ij} = \int_{\alpha_{i-1}}^{\alpha_i} \int_{\alpha_{j-1}}^{\alpha_j} s_i \, s_j \, F(\xi, \xi') \, d\xi \, d\xi' .$$

Here $s_i$ measures distance along the ith edge of the polygon. Thus, after three double quadratures over $0 \leq \xi, \xi' \leq 1$, and $4n^4$ multiplications, one can compute all the $T_{\kappa\lambda}$.

## 4. Calculation of the $I_i$.

The approximate evaluation of the $I_i$ is a non-trivial problem, because the integrand $1/|R(\xi)|$ has algebraic singularities at the interval endpoints $\alpha_0, \ldots, \alpha_n$. If the ith segment of the $\xi$-axis is divided into $2m_1$ (say 40 or 80) subintervals of length h, then the following approximate formulas are recommended.

$$(G5) \qquad \int_0^{2h} \xi^{-\mu} f(\xi) d\xi = (2h)^{1-\mu}[k_0 f(0) + k_1 f(h) + k_2 f(2h)] ,$$

where

$$k_0 = \frac{1}{1-\mu} - \frac{4}{(2-\mu)(3-\mu)} , \quad k_1 = \frac{4}{(2-\mu)(3-\mu)}$$

$$k_2 = \frac{1-\mu}{(2-\mu)(3-\mu)} ,$$

and

$$(G6) \qquad \int_{2h}^{4h} \xi^{-\mu} f(\xi) d\xi = h[k_2' f(2h) + k_3 f(dh) + k_4 f(4h)] ,$$

where $k_2'$, $k_3$, $k_4$ are analogous expressions. These formulas are exact

if $f(\xi)$ is a quadratic polynomial; thus their relative error is $O(h^{3-\mu})$.

Somewhat more tedious is the evaluation of the $\partial I_i/\partial \alpha_j$. We have here $2(n-1)^2$ indefinite single integrals to be taken over one segment. Here a somewhat less fine subdivision of each segment (into 20 or 40 subintervals) is required. The formulas of Sec. 2 reduce the singularities to those of the type treated in Eqs. G5 and G6.

## 5. Calculation of the $I^{ij}$, $J^{ij}$, $K^{ij}$.

The bulk of the computation concerns the $2n(n-1)$ coefficients $I^{ij}$, $J^{ij}$, $K^{ij}$, used in evaluating the $T_{\kappa\lambda}$. Each of these is a double integral over a product of two segments. We recommend that these be evaluated with somewhat coarser subdivisions into, say, 20 intervals on each segment. We have tried the integration, using iterated integrals. Thus we have defined

$$p_i(\xi) = \int_{\alpha_{i-1}}^{\alpha_i} \frac{\mathrm{Ln}\,|\xi - \xi'|}{R(\xi)}\, d\xi ,$$

so that

$$I^{ij} = \int_{\alpha_{i-1}}^{\alpha_i} \int_{\alpha_{j-1}}^{\alpha_j} \frac{\mathrm{Ln}\,|\xi - \xi'|}{R(\xi)\,R(\xi')}\, d\xi\, d\xi' = \int_{\alpha_{j-1}}^{\alpha_j} \frac{p_i(\xi')}{R(\xi')}\, d\xi' .$$

The second integration is quite smooth, and can be done using Simpson's Rule.

When $i = j$, the first integral involves a logarithmic singularity, combined with the algebraic singularity already discussed; the same difficulty occurs with the $J^{ii}$ and $K^{ii}$. Thus we may distinguish several cases.

(i) On the square of an interior interval, a simple logarithmic singularity occurs.

(ii) On the square of an end-interval, both logarithmic and an algebraic singularity occur.

(iii) On the product of an end-interval with a non-adjacent interior interval, where a purely algebraic singularity occurs, use Eq. G5.

(iv) On the product of an end-interval with an adjacent interior interval, a weaker singularity occurs.

We have not decided on a final integration formula for these cases, but elementary functions will commonly suffice. Thus, consider

$$\int_0^{2h} \mathrm{Ln}\, x\, f(x)\, dx = h[H_o f(0) + H_1 f(h) + H_2 f(2h)] \quad .$$

Solving from the equations

$$H_o + H_1 + H_2 = 2h(\mathrm{Ln}\, 2h - 1) \ ,$$

$$H_1 + 2H_2 = \int_0^{2h} x\, \mathrm{Ln}\, x\, dx \ ,$$

$$H_1 + 4H_2 = \int_0^{2h} x^2\, \mathrm{Ln}\, x\, dx \ ,$$

one gets elementary expressions for $H_o$, $H_1$, and $H_2$.

However, this work has not been completed.

6. Case $\rho' > 0$.

Using the preceding formulas, we have estimated that about $10^8$ multiplication times would be required to carry one problem for 100 time intervals, in the case $\rho' = 0$. Due to the artificiality of the constraints, no great accuracy could be hoped for. (The modification of Sec. 30 of LA-1862 has not been thoroughly explored.)

The case $\rho' > 0$ would involve even more time. It is, however, perhaps of interest to sketch a possible treatment of it, obtained by embedding the system in one having 3n-3 degrees of freedom, subject to n-1 workless constraints.

The original independent variables fall into three categories. First, we have the "turning angles" $\pi\mu_i$ of the case $\rho' = 0$ for the upper liquid. The corresponding angles for the lower liquid will then be

(G7) $$\mu'_i = -\mu_{n-i} .$$

Second, we have the parameters $\alpha_i$ of Sec. 10 of LA-1862. And lastly, we have corresponding parameters $0 < \alpha'_1 < \cdots < \alpha'_{n-1} < 1$ for the lower liquid; evidently, $\alpha_i$ and $\mu'_{n-1}$ are associated with the same vertex $z_i = x_i + iy_i = z'_{n-i}$.

For given $\alpha'_i$, $\mu'_i$, variables h' and A' corresponding to the h, A of Secs. 1 to 5 can be calculated by Eqs. 43 and 43' of LA-1862,

in primed variables. From these, lengths $\ell'_i$ can be calculated by Eq. 42, using primed variables. Our (n-1) constraints are then expressed by

(G8) $$\ell'_i = \ell_{n+1-i}, \qquad (i = 1, \ldots, n) ;$$

the nth condition is redundant, and can be used as a check on the calculation of A and h.

For given $\alpha'_i$, $\mu'_i$, and hence $\phi_i$, A', h', $\ell_i$, and resulting $x_i$ and $y_i$, one can compute matrices $a'_{i\lambda}$ and $b'_{i\lambda\xi}$ using analogs of formulas for the case $\rho' = 0$, in primed variables. Having these, one can compute the kinetic energy tensor $\frac{1}{2} T'_{\kappa\lambda}(\vec{q'})\ \dot{q}_\kappa \dot{q}'_\lambda$ for the lower liquid, by using analogs of the formulas of Sec. 3, and then multiplying by $\sigma = \rho'/\rho$, the relative density of the lower liquid. The sum

(G9) $$\frac{1}{2} T_{\kappa\lambda}(\vec{q'})\ \dot{q}_\kappa \dot{q}_\lambda + \frac{1}{2} \sigma T'_{\kappa\lambda}(\vec{q'})\ \dot{q}'_\kappa \dot{q}'_\lambda$$

then represents the kinetic energy of our system.

It remains to obtain an analog of the system of differential equations (29a) of LA-1862, for the Lagrangian system defined by Eq. G9, the potential energy

(G10) $$V = V(\vec{q}) - \sigma V'(q') ,$$

and the (n-1) workless constraints (G8). As the procedure for computing such an analog explicitly is hard to find in the literature, we shall sketch a non-rigorous derivation of the formulas in question. In doing

this, we shall change notation, lumping together all coordinates in the vector q.

The differentiated form of the constraint equations (G8) gives

(G11) $$(\partial \ell_i / \partial q_k - \partial \ell'_{n+1-i} / \partial q_k)\, \dot{q}_k = 0,$$

where repeated indices indicate summation. For "initial conditions" satisfying Eq. G11, the constraint conditions are equivalent to

(G12) $$0 = (\partial \ell_i / \partial q_k - \partial \ell'_{n+1-i} / \partial q_k)\, \ddot{q}_k$$

$$+ (\partial^2 \ell_i / \partial q_j \partial q_k - \partial^2 \ell'_{n+1-i} / \partial q_j \partial q_k)\, \dot{q}_j\, \dot{q}_k.$$

(Note that the nth of these is redundant, and a linear combination of the others.) The way to satisfy Eq. G12 is to introduce workless "constraint forces". The problem is to determine, in configuration space, the acceleration $\ddot{q}^*$ perpendicular to the "constraint hypersurface" which would arise from Eqs. G9 and G10, if the constraint forces were ignored. Writing

$$G_{ik} = (\partial \ell_i / \partial q_k - \partial \ell'_{n+1-i} / \partial q_k),$$

the condition that the $\ddot{q}^*$ be "workless" is that

(G13) $$G_{ik}\dot{q}_k = 0 \quad \text{imply} \quad \dot{q}_\kappa\, T_{\kappa\lambda}\, \ddot{q}^*_\lambda = 0.$$

That is, not only must the $\ddot{q}^*$ do no work, but they cannot affect

$d(T_{\kappa\lambda}\,\dot{q}_\kappa\,\dot{q}_\lambda)/dt$ for <u>any</u> motion tangent to the constraint surface. (We have not checked this non-rigorous argument critically, but it seems very plausible.)

Clearly, Eq. G13 means that $T_{\kappa\lambda}\,\ddot{q}^*_\lambda$ is a linear combination $T_{\kappa\lambda}\ddot{q}^*_\lambda = c_i G_{i\kappa}$ of the $G_{i\kappa}$; there is only one such linear combination which will imply Eq. G11; to determine this is a straight-forward problem in linear algebra. The final equations are then

$$T_{\kappa\lambda}\,\dot{q}_\kappa\,\ddot{q}_\lambda + (\kappa\lambda,\mu)\,\dot{q}_\kappa\,\dot{q}_\lambda = \partial V/\partial q_\mu + T_{\kappa\lambda}\,q_\kappa\,\ddot{q}^*_\lambda. \tag{G14}$$

## APPENDIX H

## GLOBULE ACCELERATION

Report LA-1862 dealt primarily with plane interfaces, and with spherical and cylindrical cavities. A few observations will be made here about the acceleration of "globules," i.e., of density inhomogeneities of finite extent.

The general theory of the initial acceleration of such "globules" has been given in Appendix B. The method of Appendix G can be extended to this case, provided the periodic singularity $W = \text{Ln sin } z$ is replaced by $W = \text{Ln } z$, and the effects of this change followed up. However, some other procedures can also be used.

As remarked in LA-1862 (Sec. 6), the initial acceleration of ellipsoidal globules is rigid, and so can be treated by the known* "virtual mass" methods for treating the inertial motion of solid ellipsoids in an ideal fluid. The formulas can also be extended to elliptic cylinders (Ref. 11 of LA-1862, Sec. 71), and presumably to parabolic cylinders and paraboloids.

Let an ellipsoidal globule R of density $\rho$ and volume V, in a fluid of density $\rho'$, be accelerated from rest by a gravity field of intensity g, parallel to one of the axes of the ellipsoid. The initial

*Ref. 11 of LA-1862, Chs. V and XII. See also the article by Max M. Munk in Vol. 1 of W. F. Durand, "Aerodynamic theory," Berlin, J. Springer, 1934-36 (reprinted, Durand, 1943).

rigid acceleration $a$ of $R$ will be parallel to the axis, and determined from the induced mass $\rho'M$ of $R$ as follows.

The gain in potential energy after time $t$ is $\frac{1}{2} at^2 g(\rho - \rho') V$, while the kinetic energy is $\frac{1}{2} (\rho V + \rho' M) a^2 t^2$. This gives the energy equation

$$r = \frac{a}{g} = \frac{\rho - \rho'}{\rho + \rho' M/V} = \frac{1 - \rho'/\rho}{1 + \rho' M/\rho V} . \tag{H1}$$

Thus, for fixed $R$, $\frac{a}{g}$ is a <u>linear fractional</u> function of $\rho'/\rho$ and $\lambda$, in the case of ellipsoidal globules.

From Eq. H1, and known formulae for the virtual mass of elliptic cylinders and ellipsoids, one can easily determine $a/g$ for such globules. Thus for an ellipse (Ref. 11 of LA-1862, pp. 84-5), $M = \pi a^2$, where $a$ is the transverse semi-axis, and $V = \pi ab$. Hence if $\beta = b/a$ is the <u>ratio</u> of axes, we get for the initial acceleration,

$$a = g(\rho - \rho')/(\rho\beta + \rho'). \tag{H2}$$

As $\beta \longrightarrow 0$, thus $a \longrightarrow 0$; as $\beta \longrightarrow \infty$, $a \longrightarrow g(1 - \rho'/\rho)$. Hence a long, light elliptic cylinder can be given an arbitrarily large initial acceleration, provided the density ratio $\rho/\rho'$ is sufficiently small. (This corresponds to the very intense field inside a long, slender paramagnetic rod.)

For a spheroid or ellipsoid, similar qualitative results are valid, but the formula for $M$ is more complicated. It is, for spheroids (Ref. 11 of LA-1862, p. 153).

(H3) $$M/\rho' V = \frac{a_o}{2 - \alpha_o}, \quad \text{where} \quad \alpha_o = ab^2 \int_o^\infty \frac{d\lambda}{(a^2 + \lambda)^{3/2}(b^2 + \lambda)} .$$

From Eqs. H1 and H3, we get directly

$$r = \frac{a}{g} = \frac{(2 - \alpha_o)(\rho' - \rho)}{(2 - \alpha_o)\rho + \alpha_o \rho'} .$$

A nomogram of $r$ as a function of $\rho'/\rho$ and $a/b$ is shown as Fig. 1 for spheriods with a semi-axis of symmetry of length $a$, and transverse semi-axes $b = c$.

In applying this nomogram, it should be remembered that the acceleration is $ng(r - 1)$ in the laboratory frame.

For ellipsoids, it is known that

(H3') $$M/V\rho' = \frac{a_o}{2 - \alpha_o}, \quad \text{where} \quad \alpha_o = abc \int_o^\infty \frac{d\lambda}{(a^2 + \lambda)k_\lambda}$$

and $$k_\lambda = \sqrt{(a^2 + \lambda)\,(b^2 + \lambda)\,(c^2 + \lambda)} .$$

Some numerical values for $M/V\rho'$ are shown in the following tables:

$a = 1$

| c \ b | 1 | 3/4 | 1/2 | 1/4 |
|---|---|---|---|---|
| 1 | 0.5 | 0.42 | 0.31 | 0.18 |
| 3/4 | 0.42 | 0.35 | 0.27 | 0.16 |
| 1/2 | 0.31 | 0.27 | 0.21 | 0.13 |
| 1/4 | 0.18 | 0.16 | 0.13 | 0.04 |

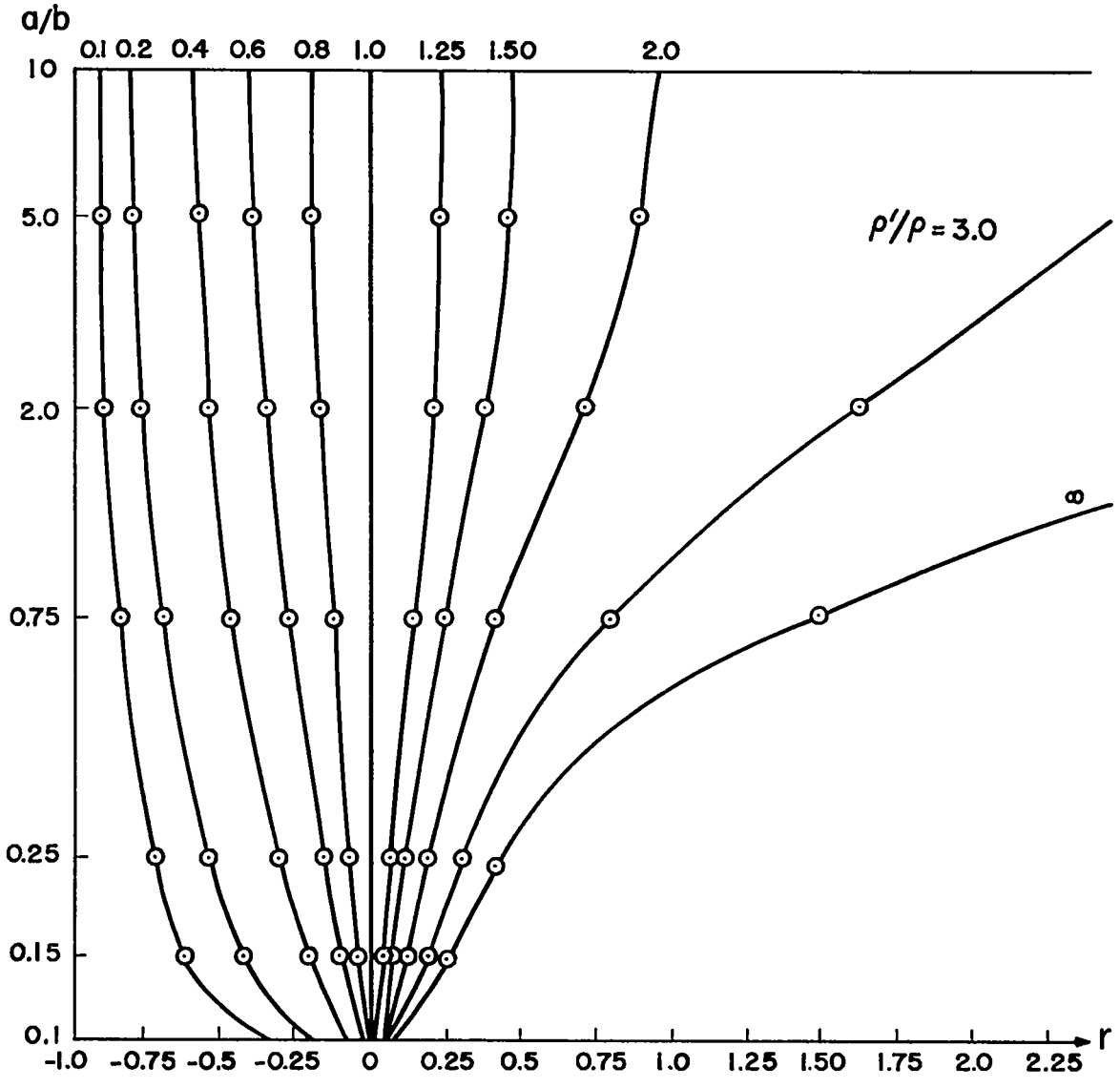
a/b
0.1 0.2 0.4 0.6 0.8 1.0 1.25 1.50 2.0
10
5.0
2.0
0.75
0.25
0.15
0.1
ρ'/ρ = 3.0
∞
r
-1.0 -0.75 -0.5 -0.25 0 0.25 0.5 0.75 1.0 1.25 1.50 1.75 2.0 2.25

Fig. 1

$a = 1/2$

| c \ b | 1 | 3/4 | 1/2 | 1/4 |
|---|---|---|---|---|
| 1 | 1.11 | 1.00 | 0.71 | 0.41 |
| 3/4 | 1.00 | 0.80 | 0.63 | 0.38 |
| 1/2 | 0.71 | 0.63 | 0.50 | 0.31 |
| 1/4 | 0.41 | 0.36 | 0.31 | 0.21 |

$a = 1/4$

| c \ b | 1 | 3/4 | 1/2 | 1/4 |
|---|---|---|---|---|
| 1 | 2.39 | | | 0.87 |
| 3/4 | | 1.74 | | 0.82 |
| 1/2 | | | 1.11 | 0.71 |
| 1/4 | 0.87 | 0.82 | 0.71 | 0.50 |

For other globule shapes, the principle stated at the end of Sec. 4 of Appendix B applies. Namely, the initial acceleration maximizes the rate of conversion of potential energy into kinetic energy*. It is corollary that the acceleration of the globule C. G. is greater than that which would be predicted by virtual mass calculations. It is another corollary that the initial acceleration can be approximately predicted by applying the Rayleigh-Ritz method to a judiciously chosen set of "trial" acceleration potentials.

Finally, it is interesting to make a rough analysis of the observed behavior of a continuously accelerated spherical globule of

*For extensions of this principle, see G. Birkhoff, "Induced potentials," von Mises Anniversary volume, Academic Press, 1954.

density $\rho'$ in a fluid of density $\rho$. Experimentally* it has been observed that an oil globule in water will flatten and "dish out" after a few diameters of travel; a cross section is sketched in Fig. 2.

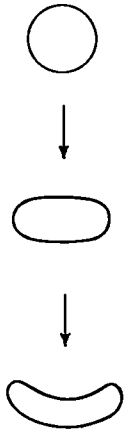

Fig. 2

The flattening is a case of Helmholtz instability, and due to the underpressure at the equator. If $a$ is the acceleration at infinity, then the initial relative acceleration of the globule is

$$a_1 = 2(\rho - \rho')\, a/(\rho + 2\rho') \qquad \alpha = 4\alpha a/(3 - \alpha)$$

After a short time $t$, the globule will have a relative velocity $a_1 t$ and an associated underpressure on the equator (relative to the stagnation pressure at the poles) of $\frac{1}{2}\rho a_1^2 t^2 = \rho a_1 s$, where $s$ is the distance travelled. The term corresponding to Taylor instability, i.e., the hydrostatic pressure difference between the poles associated with

*See G. Birkhoff and T. E. Caywood, "Fluid flow patterns," J. Appl. Phys. 20 (1949) p. 659, Fig. 15. Unpublished photographs show the effect much more clearly.

the virtual gravity, is $(\rho - \rho')$ ad. The ratio of the two is therefore

$$(H4) \qquad \frac{\text{Helmholtz}}{\text{Taylor}} = \frac{2\rho s}{(\rho + 2\rho')d} = \frac{s}{d}\,\frac{2\rho}{\rho + 2\rho'} \leqq \frac{2s}{d}\,.$$

We do not know, even qualitatively, why the globule should dish out.